National Centre for Earth Observation

NATURAL ENVIRONMENT RESEARCH COUNCIL

RESEARCH HIGHLIGHTS 2016

CONTENTS

Cover: Sentinel 3 - credit ESA/ATG media

FOREWORD

Welcome to this year's research highlights from the National Centre for Earth Observation (NCEO).

NCEO is a NERC research centre whose vision is "Transformational Earth observation (EO) science capability to meet Earth System challenges". With more than 80 scientists across leading UK universities and research organisations we provide the UK with expertise in EO science:

- Critical historical and new observations of Earth System evolution;
- Model-data evaluation for global Earth System Modelling and component models;
- Innovation data assimilation for Earth state representation and interrogation;
- Provision of instruments, data facilities and key tools for use by the wider NERC community.

We are passionate about the importance of our research to society: EO science is increasingly beneficial for a range of applications.

Within this brochure you will find articles about recent journal publications by NCEO scientists. These illustrate our current scientific goals. Topics are arranged according to science areas:

- Using Climate Datasets to understand the Earth System;
- Measuring and understanding Atmospheric Pollution and Land Emissions;
- Quantifying and understanding the Carbon Cycle: land, atmosphere and oceans;
- Observing and understanding the Energy and Water Cycles;
- Developing Data Assimilation and environmental forecasting.

Data acquisition and analysis is important to NCEO's work. The Centre for Environmental Data Analysis (CEDA) is producing the NCEO Data Management Plan, collating information on all datasets produced under NCEO. Chapter 6 of this brochure demonstrates the many uses of these datasets held on the JASMIN-CEMS infrastructure, as well as giving examples of work supported by the NERC Earth Observation Data Acquisition and Analysis Service and Field Spectroscopy Facility.

NCEO has the remit to act as champion for the wider academic community in its use of EO. There is much work to do in this space, particularly to support the continued funding of ESA's Earth Observation Envelope Programme. With this in mind, NCEO dedicated part of its 2016 Science Conference to Copernicus Science and Future Missions. Taking place shortly after the result of the Referendum on Britain's Membership of the EU, we were pleased to welcome people from the UK Space Industry and EO data community to reaffirm our commitment to collaboration.

As part of international collaboration, NCEO hosts the UK's joint GEO/CEOS Office on behalf of the UK EO community to interface to two major international initiatives: the Group on Earth Observations (GEO) and the Committee on Earth Observation Satellites (CEOS). GEO is a voluntary partnership of governments and organisations wherein decisions and actions are informed by coordinated, comprehensive EO information. It is leading a worldwide effort to create a data portal called the 'Global Earth Observation System of Systems' (GEOSS) to link EO resources worldwide across Societal Benefit Areas. CEOS is a mechanism to coordinate civil space-based EO programmes. Alongside Defra and the UK Space Agency, NCEO is working to increase the visibility of GEO to the UK EO community, facilitating and coordinating the UK's inputs to GEOSS. You can read more about this on page 36.

Supporting the training and careers of young scientists is at the heart of what we do. NCEO offers training courses to PhD students through its partnership with NERC Doctoral Training Partners and Centres for Doctoral Training. NCEO acts as a CASE partner to PhD studentships and funding-partner for the CDT in Maths for Planet Earth. Annually, NCEO runs a Researchers Forum for early career scientists in EO, where they meet fellow early career scientists from around the UK, building the network of UK EO practitioners. On pages 38-39 you can read articles based on prize-winning presentations given by 2 NCEO early career scientists at NCEO's conference.

NCEO works with partners to deliver public engagement. NCEO scientists joined NERC Centres at the Into the Blue events on RRS Discovery in Liverpool and at Manchester Airport's Visitor Centre for an exhibition of science to the public. NCEO has brought EO into classrooms through our "EO Detective" competition and teaching resources – part of the UK Space Agency's Principia project for Tim Peake's trip to the International Space Station. The winners' photographs are on pages 42-43.

We are now two years into our new five year science programme, and we are happy that 2016 has proved very productive scientifically. We hope you enjoy the highlights in this publication.

John Remedios

NCEO Director

DECADAL REANALYSIS OF A SHELF-SEA BIOGEOCHEMISTRY

Stefano Ciavatta,
NCEO and Plymouth Marine Laboratory

We performed the first decadal reanalysis simulation of the North West European (NWE) shelf-sea biogeochemistry to evaluate established indicators of ecosystem health and to quantify climate-relevant carbon fluxes. Earth Observations of ocean colour were assimilated into a marine ecosystem model of the shelf ecosystem to implement a reanalysis spanning years 1998–2009. Skill and confidence of the outputs were quantified. We found that large areas of near-bed shelf waters were oxygen deficient, potentially threatening bottom fish and benthic communities. The reanalysis showed that the shelf is a net sink of atmospheric carbon dioxide (CO_2).

Methodology

The marine model of the NWE shelf couples the hydrodynamic model POLCOMS (Holt and James, 2001) with the ecosystem model ERSEM (Butenschön et al., 2016). We assimilated ocean colour by using a stochastic, localised Ensemble Kalman filter (EnKF) (Evensen, 2003) with an ensemble size of one-hundred model simulations. We assimilated remotely sensed concentrations of surface chlorophyll, provided by the Ocean Colour – Climate Change Initiative project of the European Space Agency (Sathyendranath et al., 2016). The assimilation scheme used per-pixel error statistics available with the ocean colour product. The skill of the reanalysis was assessed by using robust non parametric statistics with in situ physical and biogeochemical observations from the Ecosystem Data Online Warehouse of the International Council for the Exploration of the Sea (www.ices.dk) and the Surface Ocean CO_2 Atlas (Bakker et al., 2014; http://www.socat.info/). The percentiles of the ensemble distribution defined the confidence levels of the output.

Key results and impacts

The reanalysis improved the model simulation of ocean colour chlorophyll in the majority of the study region. The simulation was highly skilled in estimating in situ data of temperature, salinity, and dissolved oxygen, and it had some skill for in situ chlorophyll, nutrients and partial pressure of CO_2. We found that between 325,000–365,000 km^2 of shelf bottom waters were vulnerable to oxygen deficiency, i.e. their minimum oxygen concentration fell at least once below the 6 mg L^{-1} threshold defined by the OSPAR Commission to protect the North East Atlantic ecosystem (Figure 1a). The reanalysis showed that the shelf is a net sink of atmospheric CO_2, but estimates of the total uptake range between 36 and 46 Tg C yr^{-1} at a 90% confidence level (Figure 1b). The provision of confidence levels, along with skilled biogeochemical estimates, was recognised a major contribution of this work to inform marine policy and climate studies (Cook, 2016). Currently, the reanalysis product is being used to develop the operational forecasting system at UK Met Office, as well in other projects of the European Copernicus Marine Environment Monitoring Service and Horizon2020 Programmes, e.g. for planning sustainable aquaculture in European seas. The product is freely available to end users via a public data portal (https://portal.ecosystem-modelling.pml.ac.uk).

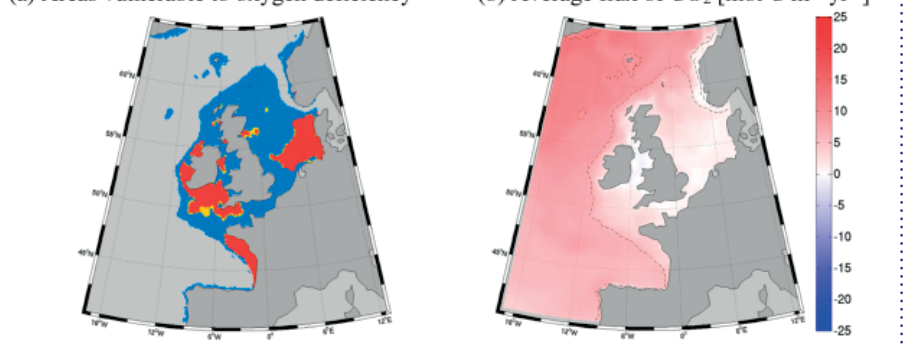

Figure 1. Applications of the reanalysis product for marine policy and climate studies. (a) Map of bottom shelf areas vulnerable to oxygen deficiency: yellow colour represents deficient areas at 1% confidence level (i.e. at least one member of the ensemble signals oxygen deficiency on at least one day in the simulation), red represents 100% confidence (all the one-hundred members signal deficiency), and blue are shelf areas with concentration higher than 6 mg L-1 at 100% confidence. (b) Average yearly values of air-sea flux of CO2 in the period 1998-2009 positive values represent sink, negative values source); the dashed line represents the 200 m isobath delimiting the shelf region for convention.

Featured publication

Ciavatta, S., S. Kay, S. Saux-Picart, M. Butenschön, and J. I. Allen (2016), Decadal reanalysis of biogeochemical indicators and fluxes in the North West European shelf-sea ecosystem, *J. Geophys. Res. Oceans*, 121, 1824–1845, doi: 10.1002/2015JC011496.

Additional science references

Bakker, D. C., at al. (2014), An update to the Surface Ocean CO2 Atlas (SOCAT version 2), *Earth Syst. Sci. Data*, 6 (1), 69–90.

Butenschön, M., et al., (2016), ERSEM 15.06: a generic model for marine biogeochemistry and the ecosystem dynamics of the lower trophic levels, *Geosci. Model Dev.*, 9, 1293–1339, doi:10.5194/gmd-9-1293-2016.

Cook, T. (2016), Uncertainty evaluations improve biogeochemical simulations, *Eos*, *97*, doi:10.1029/2016EO047765.

Evensen, G. (2003), The Ensemble Kalman Filter: theoretical formulation and practical implementation, *Ocean Dynam.*, 53(4), 343–367, doi:10.1007/s10236-003-0036-9.

Holt, J. T., and I. D. James (2001), An s coordinate density evolving model of the northwest European continental shelf – 1, Model description and density structure, *J. Geophys. Res.*, 106(C7), 14015–14034.

Sathyendranath, S., et al. (2017), Ocean-colour products for climate-change studies: What are thier ideal characteristics?, *Remote Sens. Environ.*, 203, 125-138.

TESTING A NEW GLOBAL MAP OF VEGETATION AMOUNT AND PRODUCTIVITY

Mathias Disney, NCEO UCL

Terrestrial vegetation is often characterised via two properties, the leaf area index (LAI) and the fraction of absorbed photosynthetically radiation (fAPAR). The first is a measure of vegetation amount, the second of photosynthetic efficiency. These properties are widely-derived from EO and used in models of climate and the carbon cycle. But different products differ strongly, leading to large model prediction uncertainties. We present a new product designed with these kinds of models in mind, and we show how important it is to make assumptions in both the satellite products and the models, explicit. Our product is freely available and ought to help improve global carbon cycle model predictions.

Methodology

GlobAlbedo is a synthesis of EO data from various sources from 2002 onwards, combined using a data assimilation approach, into an estimate of albedo (surface reflectivity) at 1km scale, with uncertainty. As a by-product, we have used GlobAlbedo to estimate LAI and fAPAR, using a relatively simple scheme describing how radiation interacts with vegetation. Crucially, the model was designed explicitly for global parameter retrieval from albedo, and is consistent with both the observations **and** the type of large-scale climate, carbon model they are designed to be used in. This is in contrast to other EO-derived estimates of LAI and fAPAR, which are derived either purely empirically, or using methods purely designed for satellite retrievals. We compare the GlobAlbedo LAI and fAPAR products with a widely-used alternative from the NASA MODIS instrument. We quantify some of the similarities and differences in space and time between the two products, across a range of biomes and cover types and we discuss why these differences arise. Our aim is not to determine 'the best' product per se, but to highlight and explain these differences in terms of the underlying models and assumptions, and point out the implications for this in global modelling activities.

Key results and impacts

We show that the GlobAlbedo fAPAR and LAI values are temporally more stable than MODIS values due to the smoothness of the underlying albedo. The parameters agree closely in timing but GlobAlbedo values are consistently lower than their MODIS counterparts, particularly for LAI. Differences arise due to the assumptions underlying the products, meaning care is required in interpreting either set of values, particularly when comparing to fine-scale ground-based estimates. We present global transformations between the GlobAlbedo-derived and MODIS products. GlobAlbedo data are freely available and are being used to improve climate model simulations, by the Met Office for example; these products are also likely to improve carbon cycle model predictions.

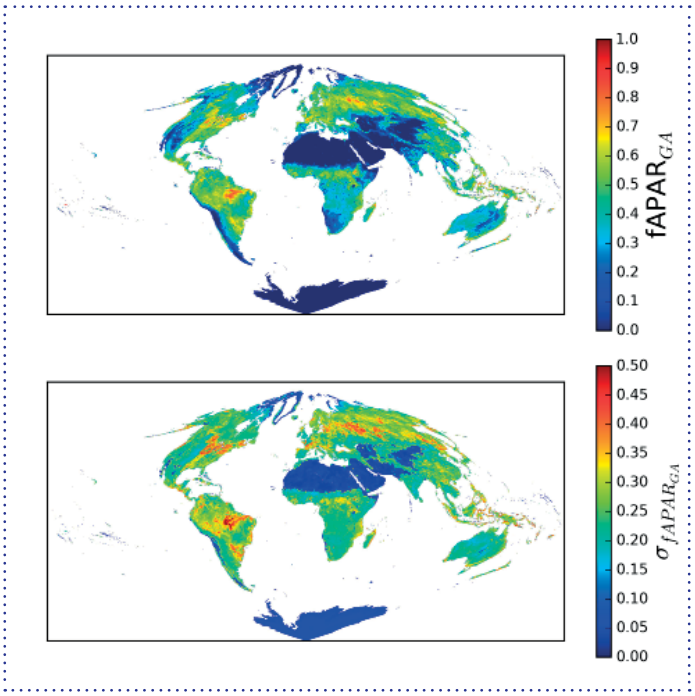

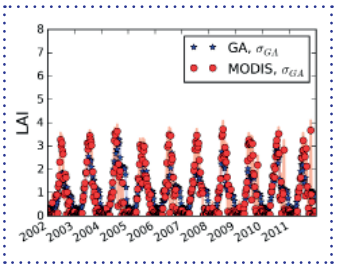

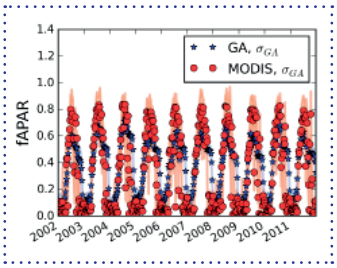

Figures. Grasslands' leaf area indix and fraction of absorbed photosynthetically radiation.

Featured publication

Disney, M. I.; Muller, J.-P.; Kharbouche, S.; Kaminski, T.; Voßbeck, M.; Lewis, P.; Pinty, B. A New Global fAPAR and LAI Dataset Derived from Optimal Albedo Estimates: Comparison with MODIS Products. *Remote Sens.* 2016, 8, 275, doi: 10.3390/rs8040275. GlobAlbedo: http://www.globalbedo.org/.

Acknowledgment
Data were funded via ESA WACMOS contract #4000106711/12/I-NB and ESA GlobAlbedo contract# 22390/09/I-OL, led by J.-P. Muller at UCL-MSSL. Analysis tools were developed using NCEO and EU-FP7 QA4ECV funding (Project No 607405) at UCL-MSSL by S. Kharbouche. M. Disney was supported in part via NCEO, NERC GREENHOUSE (NE/K002554/1) and EU H20:20 BACI project (Project No. 640176).

OCEAN HEAT CONTENT FROM OCEAN REANALYSES

Keith Haines, NCEO Reading

Ocean ReAnalyses (ORA) use dynamical models to assimilate observations distributed in space and time into a consistent 4D reconstruction of the evolving ocean state. Recovering ocean heat content (OHC) and how it changes is key to understanding the Earth's energy budget. This is one of 9 international collaborative papers comparing reanalysis products from around the world. The ensemble mean (±sigma) of rolling 5-year OHC trends shows relatively steady heat uptake ~0.9 ± 0.8 W m^{-2} (relative to the whole Earth's area) from 1995–2002, reducing to ~0.2 ± 0.6 W m^{-2} from 2004-2006, in reasonable agreement with recent independent analyses.

Methodology

Nineteen products were assessed, three of which used only statistical interpolation. Signal to noise for seasonal and interannual variability and for OHC trends were assessed e.g. by comparing ensemble mean temporal variability (signal) with the ensemble spread between products (noise).

Key results and impacts

Spatial patterns of interannual variability for the period 1997–2009 show good agreement in the upper 300m (Fig.1) through most of the northern hemisphere and especially the tropics where the El Nino signals dominate. There is less agreement in variability patterns at deeper levels, although the Atlantic and Southern Oceans are regions in which most ORAs show widespread warming trends below 700m, with noise being anomalously high due to large drifts in some outliers (see paper Fig. 16).

A number of ORAs exhibit enhanced global ocean heat uptake below 300 and 700 m during the mid-1990s to early 2000s, Figure 2b. These multi-product results therefore qualitatively supporting the ECMWF findings, Balmaseda et al. (2013) who suggest this maybe associated with changes in the Pacific Decadal Oscillation combined with a weakening of the Atlantic Meridional Overturning Circulation. However, it remains unclear how much of this enhanced deep ocean heat uptake might be explained as a sampling artefact because there is a dramatic improvement in sampling during the initiation of the worldwide Argo float program from 2001–2003.

Much of this increase in deep ocean heat uptake in the ORAs during the 2000s may result from Argo suddenly 'revealing' a longer-term Southern Ocean warming signal (Roemmich et al. 2015).

Studies such as these are critical for enhancing understanding of changes to the Earth's energy budget taking place

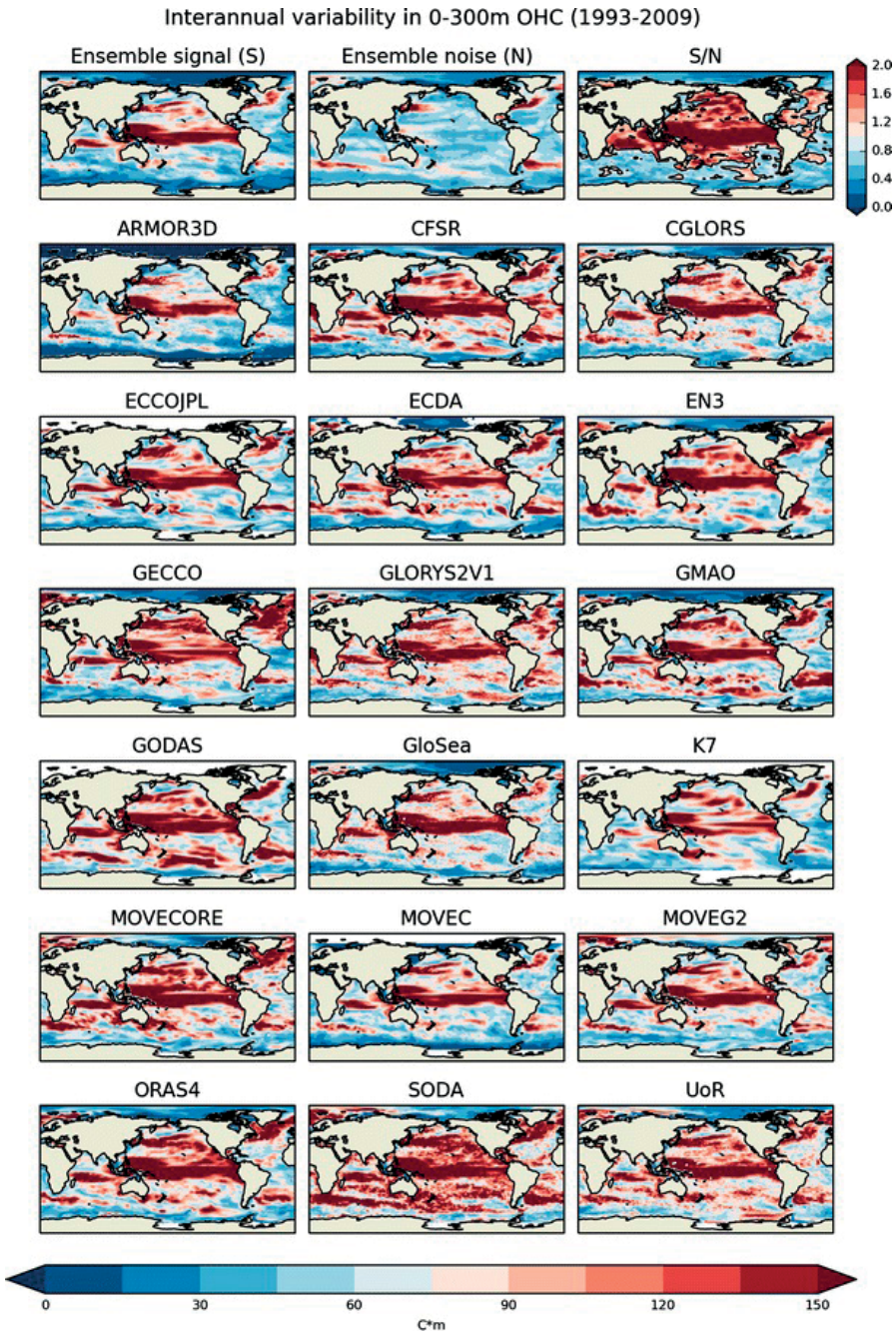

both naturally and due to anthropogenic CO_2 emissions. We are contributing to the WCRP CLIVAR program trying to improve quantification of the Earth's energy budget www.clivar.org/research-foci/heat-budget. The oceans take up nearly all of the excess heat trapped by the atmosphere but we still need to understand how this is happening. Where and at what depths are the oceans warming? Will the rate of heat uptake remain the same? Will excess heat stored at depth return back to the surface suddenly increasing the rate of surface temperature warming? Will the warmer waters, with lower densities, cause changes in ocean currents? Improved Ocean Reanalyses should help to answer some of these questions e.g. further work should assess the consistency of ocean currents and heat transports directly within the model products. Combining ocean heat transports with atmospheric heat transports and top of atmosphere satellite radiation data should help provide a more complete picture of the energy flows within the Earth system.

The standardised data products generated by this ORA Intercomparison project are now being archived for wider use at http://icdc.cen.uni-hamburg.de/1/daten/reanalysis-ocean/oraip.html. For example an ongoing project is extending the reanalysis comparison with 2 additional papers on the Arctic and Antarctic seas, covering OHC, salinities, mixed layer depths and ice distributions. The data archive will therefore provide a baseline for assessing the improvement of future reanalysis products.

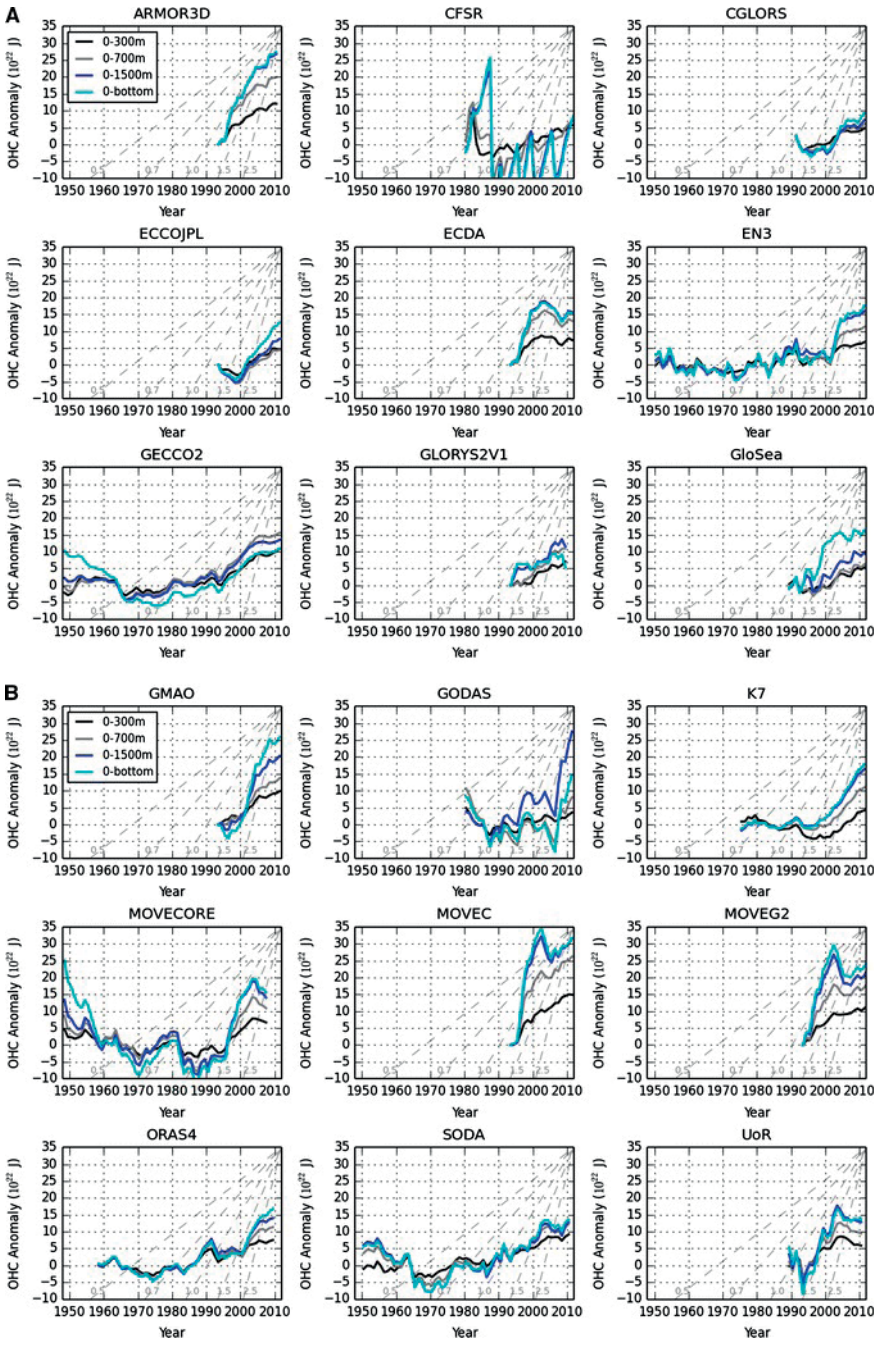

Figure 1. Interannual variability of depth-integrated temperature for the 0–300 m layer (Celsius meters) for each ORA, computed as the temporal standard deviation of annual mean values for each grid box after removing a linear trend. White areas indicate where no data are available. Also shown is the ensemble average temporal standard deviation ('signal', S), the temporal average of the ensemble standard deviation ('noise', N), and the ratio of the two (S/N). The ensemble values (top row) are computed for each grid box based on all available data. All values computed for 1993–2009 except for MOVECORE (1993–2007)

Figure 2. Time series of ocean heat content change for a range of depth intervals, computed to a baseline period of 1948–1993 for illustrative purposes. The dashed grey lines indicate the equivalent heating rate (W m^{-2}) computed for Earth's surface area.

Featured publication

Palmer M.D *et al.* Ocean heat content variability and change in an ensemble of ocean reanalyses *Clim. Dyn* doi: 10.1007/s00382-015-2801-0.

References

Balmaseda MA, Trenberth KE, Källén E (2013) Distinctive climate signals in reanalysis of global ocean heat content. *Geophys Res Lett* 40:1754–1759. doi:10.1002/grl.50382.

Roemmich D et al (2015) Unabated planetary warming and its ocean structure since 2006. Nat Clim Change. doi:10.1038/nclimate2514.

BAYESIAN ANALYSIS OF UNCERTAINTY IN THE GLOBCOVER 2009 LAND COVER PRODUCT AT CLIMATE MODEL GRID SCALE

Tristan Quaife, NCEO Reading

Land cover derived from satellites is an important input data set to climate models. Understanding how uncertainties in these data propagate through the errors in model outputs however is not trivial, in part because of the way the uncertainties in the land cover data are usually represented. We have designed a Bayesian method to enable propagation of these errors through any process based model that requires land cover as one of its input variables. Our paper (Quaife and Cripps, 2016) applies this method to the European Space Agency's GlobCover 2009 land cover data set.

Methodology

We designed a Gibbs sampler to draw from the posterior probability distribution of the uncertainty in the true land cover given the uncertainties defined in a confusion matrix and the corresponding EO derived land cover estimates themselves. The confusion matrix is the de-facto standard for recording uncertainty on EO land cover data, but is not readily propagated though process based models. We then sample from the posterior distribution to produce a large number of equally likely realisations of the EO derived land cover.

We used this method with the European Space Agency's GlobCover 2009 data set to generate 10000 equally likely realisations of the global distribution of land cover. Using this large number of land cover maps we were able to analyse various characteristics of the GlobCover data and describe situations in which it performed well and where it performed badly. The results of this exercise are summarised in Figure 1. These data can then be propagated through a model of interest and the deviations in the model outputs examined to understand the impact that the uncertainty in the land cover has on the model predictions. We are working on this currently.

Key results and impacts

The main result of our work is that the GlobCover data is a reliable representation of global land cover. Areas of uncertainty tend to correspond to heterogeneous landscapes, which reflects the difficulty of correctly classifying areas with mixed cover types from remote sensing data. We also observed that some cover types have significant biases in reported global area; in particular for permanent snow and ice areas and inland water bodies. We are currently in the process of assessing the impact of these uncertainties on the global carbon balance by propagating our realisations of land cover through a global vegetation model.

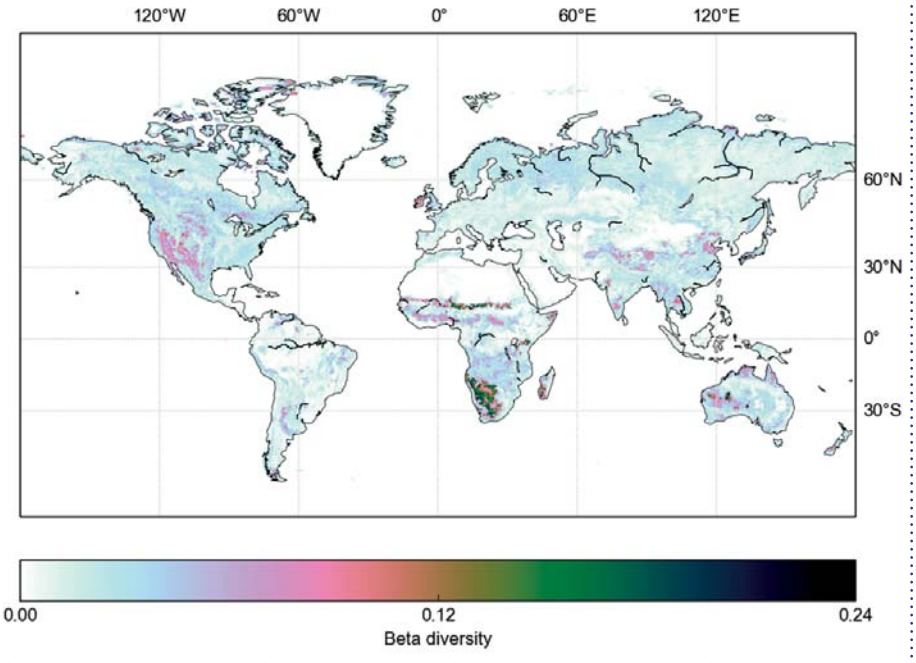

Figure 1. Uncertainty in the GlobCover 2009 data as calculated using the method described by Quaife and Cripps (2016) and summarised using the Beta diversity statistic. This figure is taken from the original manuscript, published under the Creative Commons Attribution License (CC BY 4.0).

Featured publication

Quaife T. and Cripps E. (2016) Bayesian Analysis of Uncertainty in the GlobCover 2009 Land Cover Product at Climate Model Grid Scale. *Remote Sensing.* 8(4), 314; doi: 10.3390/rs8040314.

UNDERSTANDING THE 11-YEAR SOLAR CYCLE IN STRATOSPHERIC OZONE

Dhomse Sandip and Martyn Chipperfield, NCEO Leeds

Up to now our understanding of the 11-year ozone solar cycle signal (SCS) in the upper stratosphere has been largely based on the v6.2 Stratospheric Aerosol and Gas Experiment II (SAGE II) satellite data record. This indicated a large positive signal which could not be reproduced by models, calling into question our understanding of the chemistry of that region. Here we analysed the new v7.0 SAGE II data and found a smaller upper stratosphere ozone SCS, due to a more realistic ozone-temperature anti-correlation in the new SAGE retrievals. Simulations with a state-of-the-art 3-D model show a small SCS in the upper stratosphere, in agreement with SAGE v7.0 data and other shorter term satellite records.

Methodology

Ozone in the upper stratosphere is under photochemical control and the SCS there is primarily attributed to change in solar fluxes. We used the TOMCAT 3-D chemical transport model to simulate long-term ozone changes (1979-2015) using different prescribed solar fluxes representing the 11-year solar cycle (NRL and SATIRE). The model was forced with realistic ECMWF meteorological data from the European Centre for Medium-Range Weather Forecasts (ECMWF). In collaboration with R. Damadeo and J. Zawodny of NASA Langley, we analysed two versions of SAGE II ozone data [1984-2005]. We also used ozone profiles from the Halogen Occultation Experiment (HALOE) v19 [1992-2005], Microwave Limb Sounder (MLS) v4.2 [2004-2015] and Atmospheric Chemistry Experiment (ACE) v3.5 (2005-2015]).

In the upper stratosphere the model, SAGE, HALOE, MLS and ACE data show a clear anti-correlation between ozone and temperature (Figure 1), due to the temperature-dependence of ozone loss reactions. Our results show that this relationship is better represented in the updated SAGE II v7.0 data compared to v6.2. The SCS estimated using a multivariate regression model (Figure 2) shows a much weaker SCS in the tropical upper stratosphere in the model, SAGE II v7.0, HALOE and MLS data compared to SAGE 6.2 data.

Key results and impacts

The inability of chemistry-climate models to simulate the apparently large ozone solar cycle in the upper stratosphere retrieved from the long-term SAGE II (v6.2) record was a cause of concern. It called into question our understanding of the upper stratosphere and our ability to model the 'top-down' forcing of solar variations on climate through changes in stratospheric ozone. With the availability of updated SAGE v7.0 data, we revisited this discrepancy and found a smaller SCS in upper stratospheric ozone (through improved ozone-temperature correlations), in much better agreement with models. This improves our confidence in how we can model the effects of solar flux changes on atmospheric composition and climate.

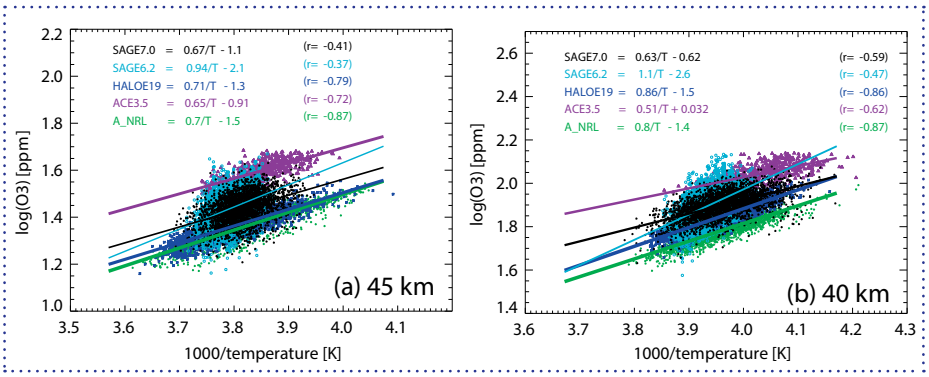

Figure 1. Variation of log (O_3 mixing ratio) versus 1000/temperature at (a) 45 km and (b) 40 km for tropical (20°S-20°N) sunset measurements from ACE (2006-2010), HALOE (1996-2000) and SAGE II (v7.0 and v6.2, 1996-2000). Also shown are TOMCAT model sunset values (run A_NRL) sampled at the SAGE II locations. The legends indicate the parameters to the linear regression fits; the thicknesses of the regression lines are scaled to the magnitude of the correlation coefficients (r).

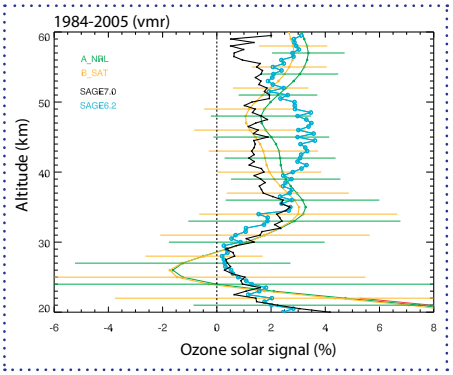

Figure 2. Vertical profiles of the estimated solar cycle signal (SCS) in stratospheric ozone vmr from TOMCAT model runs with different solar fluxes (A_NRL green; B_SAT orange) for 1984-2005. Horizontal lines show 2-σ error bars (shown every 4 km to improve the clarity). Also shown are the estimated SCS from SAGE II v7.0 (black) and v6.2 (light blue) volume mixing ratio data. No error bars are shown for SAGE data.

Featured publication

Dhomse SS; Chipperfield MP; Damadeo RP; Zawodny JM; Ball WT; Feng W; Hossaini R; Mann GW; Haigh JD (2016) On the ambiguous nature of the 11 year solar cycle signal in upper stratospheric ozone, *Geophysical Research Letters*, 43, pp. 7241–7249. doi: 10.1002/2016GL069958.

Additional science references

Dhomse SS et al., (2011) Solar response in tropical stratospheric ozone: a 3-D chemical transport model study using ERA reanalyses, *Atmos. Chem. Phys*, 11, pp.12773–12786.

TRENDS IN STRATOSPHERIC HYDROGEN FLUORIDE (HF)

Jeremy Harrison, NCEO Leicester and Martyn Chipperfield, NCEO Leeds

The vast majority of the emissions of fluorine-containing molecules into the atmosphere are anthropogenic in nature, e.g. chlorofluorocarbons (CFCs), hydrochlorofluorocarbons (HCFCs), and hydrofluorocarbons (HFCs). All CFCs and HCFCs are regulated by the Montreal Protocol because they catalytically destroy stratospheric ozone on account of their containing chlorine atoms; these molecules are also potent greenhouse gases. Of the most abundant species in the atmosphere, CFC-12 (CCl_2F_2) and CFC-11 (CCl_3F) have now been banned and their atmospheric abundances are slowly reducing, whereas HCFC-22 ($CHClF_2$) is still increasing in the atmosphere. The unregulated HFCs, which do not deplete stratospheric ozone, are also increasing.

Once released into the atmosphere, fluorine-containing molecules slowly degrade, ultimately leading to the formation of HF, the dominant reservoir of stratospheric fluorine due to its extreme stability. Monitoring the growth of stratospheric HF therefore reveals overall changes in fluorine-containing greenhouse gases in the atmosphere, and provides an important marker for the success of the Montreal Protocol. Indeed, satellite observations reveal a substantial slowing down in the rate of increase of HF since the 1990s, consistent with the reduction in emissions under the Protocol.

Methodology

Global distributions and trends of HF measured by the international satellite remote-sensing instruments ACE-FTS (Atmospheric Chemistry Experiment Fourier Transform Spectrometer), which has been recording atmospheric spectra since 2004, and HALOE (HALogen Occultation Experiment), which recorded atmospheric spectra between 1991 and 2005, were compared with the output of SLIMCAT, a UK state-of-the-art three-dimensional chemical transport model. The model chemistry was successfully tested by comparing tracer-tracer correlations for a number of major HF 'source' gases for both SLIMCAT and ACE-FTS data.

Key results and impacts

The observed global HF trends reveal a substantial slowing down in the rate of increase of HF since the 1990s: 4.97 ± 0.12 %/year (1991-1997; HALOE), 1.12 ± 0.08 %/year (1998-2005; HALOE), and 0.52 ± 0.03 %/year (2004-2012; ACE-FTS). In comparison, SLIMCAT calculates trends of 4.01 %/year, 1.10 %/year, and 0.48 %/year, respectively, for the same periods; the agreement is very good for all but the earlier of the two HALOE periods. Furthermore, the observations reveal variations in the HF trends with latitude and altitude, for example between 2004 and 2012 HF actually decreased in the southern hemisphere below ~30–35 km. An additional SLIMCAT simulation with repeating meteorology for the year 2000 produces much cleaner trends in HF with minimal variations with latitude and altitude. Therefore, the variations in the observed HF trends can be attributed to variability in stratospheric dynamics on the timescale of a few years. Overall, the broad agreement between observation and model points towards the ongoing success of the Montreal Protocol and the usefulness of HF as a metric for stratospheric fluorine.

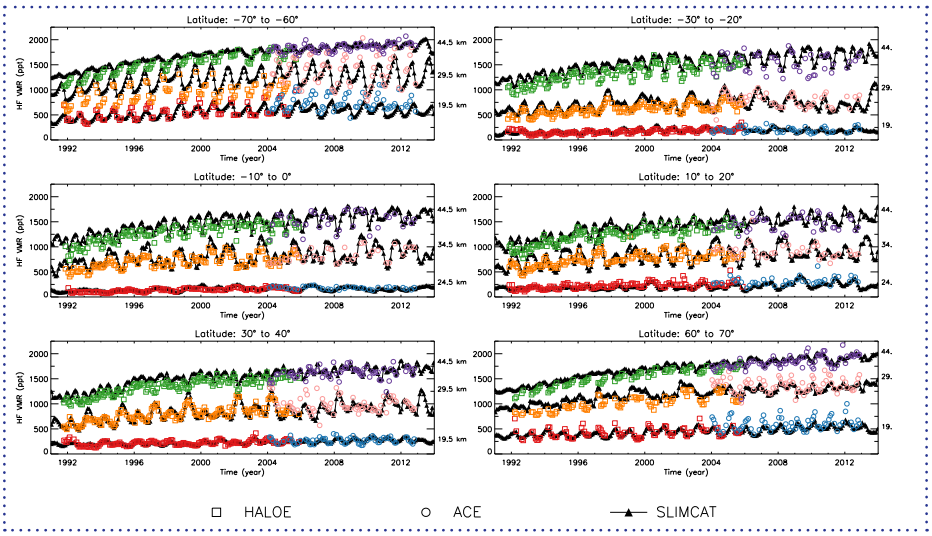

Figure 1. The HALOE, ACE-FTS and SLIMCAT HF time series for selected altitude – latitude bin combinations. Observations are plotted between October 1991 and December 2012.

Featured publication

J.J. Harrison et al., Satellite observations of stratospheric hydrogen fluoride and comparisons with SLIMCAT calculations, *Atmos. Chem. Phys.*, 16, 10501–10519, 2016, doi: 10.5194/acp-16-10501-2016.

This publication was selected as an EGU highlight article (22 August 2016).

ROLE OF OH VARIABILITY IN THE STALLING OF THE GLOBAL ATMOSPHERIC CH4 GROWTH RATE FROM 1999 TO 2006

Joe McNorton, NCEO Leeds

The growth in atmospheric methane (CH_4) concentrations over the past two decades has shown large variability on an interannual timescale. During a stagnation period from 1999 to 2006 this growth rate slowed to 0.6 ppb/yr. We have used a 3-D global chemical transport model, driven by meteorological reanalyses and variations in OH to investigate these variations. Results show changes in the CH_4 atmospheric loss contributed significantly to the suppression in global CH_4 concentrations between 1999-2006. The largest factor in this is small variations in global mean OH. These results imply a smaller variation in emissions is required to explain the observed CH_4 trends.

Methodology

We used methyl chloroform (CH_3CCl_3) measurements from two networks (NOAA and AGAGE) between 1997 and 2009 to derive global mean anomalies in the hydroxyl radical (OH). The reaction of OH with methane (CH_4) is a major atmospheric CH_4 sink (~90%), therefore variations in OH are likely to contribute to CH_4 growth variability. To investigate this we used a 3-D global chemical transport model, driven by meteorological reanalyses and variations in global mean hydroxyl (OH) concentrations. We performed multiple model CH_4 and CH_3CCl_3 simulations, using configurations of varying/repeating OH/temperature/transport. By comparing these simulations with observed CH_4 and CH_3CCl_3 we could assess both the model's ability to reproduce observed growth variability and the individual contributions of OH/temperature/transport to the CH_4 growth variability.

Key results and impacts

Results highlight the important role of OH variability in the interannual atmospheric growth rate of CH4 and in particular during the 1999–2006 stagnation period. Changes in emissions are clearly important in the growth variability, however these results imply smaller changes in emissions can explain the observed CH_4 trends. The observed growth in CH_4 since 2007 could also, in part, be explained by reduced OH; however, this cannot be fully determined with data currently available.

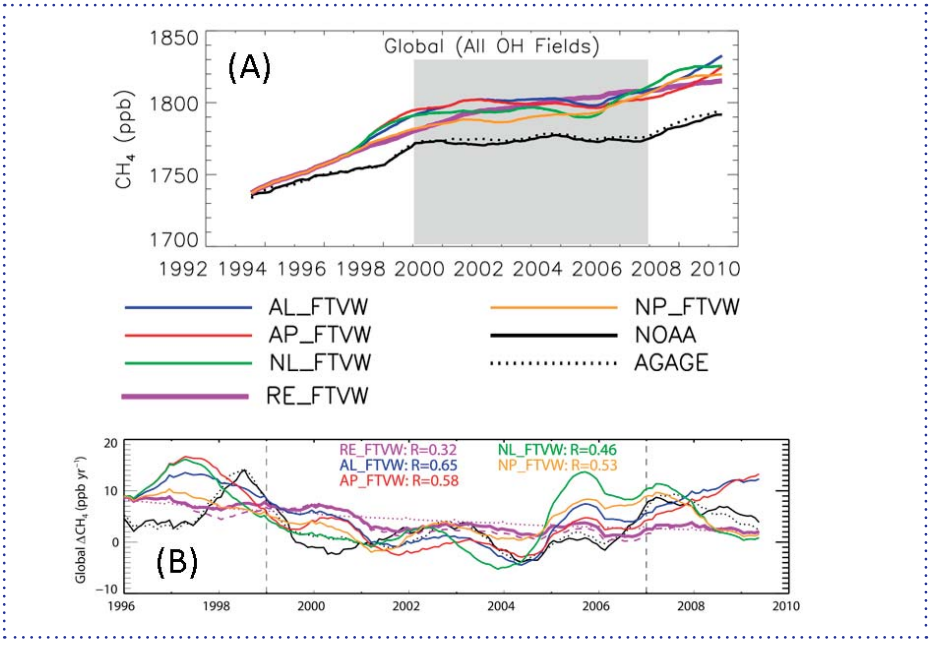

Figure 1. Deseasonalised global mean surface CH4 from NOAA (black solid) and AGAGE (black dashed) observations along with five TOMCAT simulations with different treatments of OH. The simulation with interannually repeating OH (RE_FTVW) fails to capture the observed decrease in growth between 1999 and 2006. The shaded region marks the stagnation period in the observed CH4 growth rate.

Figure 2. The global CH4 growth rate for the same observations and simulations as (A), all simulations which use varying OH (AL, AP, NL and NP) capture the observed growth rate better than the simulation using repeating OH (RE).

Featured publication

Joe McNorton, Martyn Chipperfield, Manuel Gloor, Chris Wilson, Wuhu Feng, Garry Hayman, Matt Rigby, Paul Krummel, Simon O'Doherty, Ronald Prinn, Ray Weiss, Dickon Young, Ed Dlugokencky ; Role of OH variability in the stalling of the global atmospheric CH_4 growth rate from 1999 to 2006; *Atmos. Chem. Phys.*, 16, 7943–7956, 2016; doi: 10.5194/acp-16-7943-2016.

DETECTION OF THE YORKSHIRE POWER STATIONS FROM SPACE: AN AIR QUALITY PERSPECTIVE

Richard Pope, NCEO Leeds

Over the UK there are many anthropogenic sources of pollution such as traffic, industry and power generation. Using satellite measurements of tropospheric column Nitrogen Oxide (NO_2) we can see the pollution hotspots over the UK such as London, Birmingham and Manchester. However, enhanced pollution seen over East Yorkshire has no large cities nearby. Yorkshire has three large power stations (Drax, Eggborough and Ferrybridge) which we suspected were the cause of the enhanced NO_2 seen from space. On very calm days, the satellite can see the build-up of pollution over these power stations significantly increasing local/regional pollution levels.

Methodology

Tropospheric column NO_2 data from the Ozone Monitoring Instrument (OMI), on-board NASA's AURA satellite which has a local overpass time of 13:30, was analysed between 2005 and 2011 to investigate UK pollution hotspots. Unlike London, Manchester and Birmingham, the Yorkshire hotspot had no big cities nearby. Therefore, we suspected that the large power stations in East Yorkshire might be the cause. Figures 1b and c show that Drax emitted over 40 kTonnes of NO_x ($NO + NO_2$) in some years, which is the largest single UK source based on estimates from Drax itself and the National Atmospheric Emissions Inventory (NAEI). Therefore, OMI NO_2 data were sampled over East Yorkshire on calm (<2.5 m/s) and windy (> 7.5 m/s) days. On windy days we expected pollution to be transported away from the power stations, while under calm conditions it would accumulate over the region. The calm and windy days were determined from the average of 10 m wind speeds from 16 weather stations across East Yorkshire.

Key results and impacts

Under average conditions (Figure 2a), OMI shows peak regional tropospheric column NO_2 of 8-11 x10^{15} molecules/cm^2 located over the Yorkshire power stations (black symbols). Windy conditions, which are climatologically westerly in the UK, show reduced pollution over the power stations (6-8 x10^{15} molecules/cm^2) with clear transport out towards Hull and the North Sea (Figure 2b). Figure 2c shows OMI NO_2 under the calm conditions with low wind speeds. Here the peak pollution levels are located over Drax and Eggborough of over 20 x10^{15} molecules/cm^2. As there is limited transport of pollution, this infers that these large NO_2 concentrations are caused by the direct emission of pollution from these power stations and explain the pollution hotspot seen by OMI.

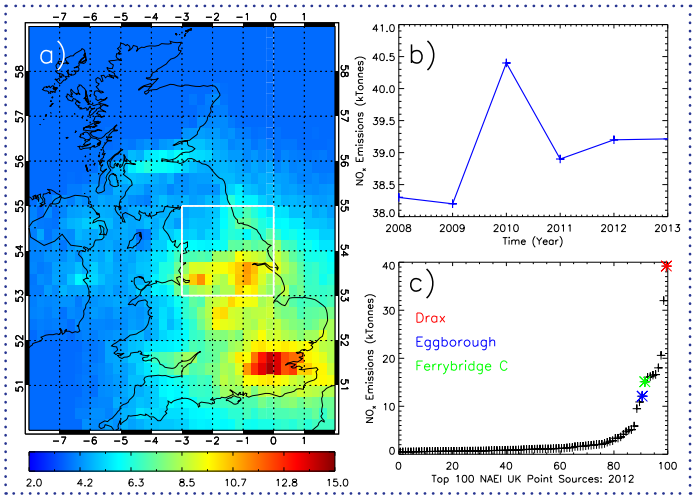

Figure 1. a) OMI tropospheric column NO_2 (x10^{15} molecules/cm^2) between 2005-2011over the UK, b) Drax NO_x emissions between 2008-2013 and c) top 100 NAEI NO_x point source emissions for 2012 (kTonnes).

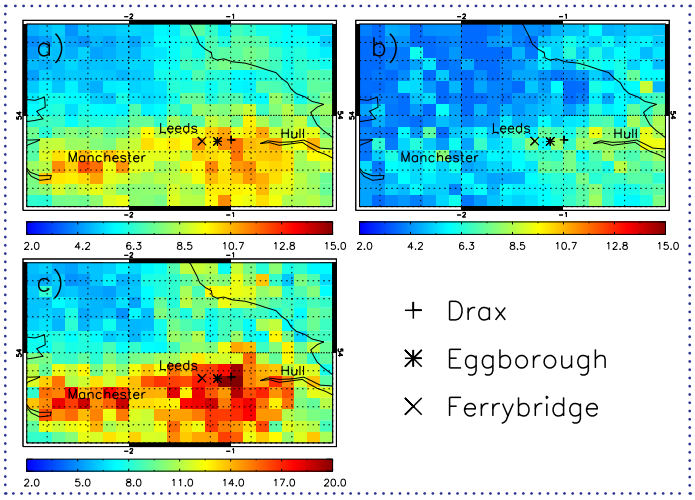

Figure 2. OMI tropospheric column NO_2 (x10^{15} molecules/cm^2), 2005-2011, over northern England: a) 7-year average, b) sampled under high wind speeds (>7.5 m/s) and c) sampled under low wind speeds (<2.5 m/s).

Featured publication

Featured publication: Pope, R.J. and M. Provod, Detection of the Yorkshire power stations from space: an air quality perspective. *Weather*, 71, 2, pp 40–43, doi: 10.1002/wea.2651, 2016.

AMAZON BASIN SHOWN TO CONTRIBUTE SIGNIFICANTLY TO GLOBAL METHANE EMISSIONS

Chris Wilson, NCEO Leeds

Until recently, atmospheric concentrations of methane (CH_4) over the Amazon Basin of South America were relatively poorly observed compared to other regions of the globe. Wetland regions in the basin were thought to contribute significantly the global natural CH_4 source, but the lack of long-term atmospheric observations across much the region has made quantification of emissions difficult. We used a new set of in-situ observations made within the Amazon since 2010, together with a 3-D atmospheric transport model, to quantify basin-wide CH_4 emissions. Our findings indicate that the Amazon contributes significantly (up to 7%) to total global CH_4 emissions.

Methodology

Since 2010, aircraft-borne flask air observations of CH_4 and carbon monoxide (CO) have been made at four Amazon sites by researchers at the Instituto de Pesquisas Energéticas e Nucleares (IPEN) in Sao Paulo, Brazil, in collaboration with the University of Leeds, UK, and the Earth System Research Laboratory of the National Oceanic and Atmospheric Administration (NOAA/ESRL) in Boulder, CO, USA. The measurement locations were chosen in order to sample the dominant tropospheric airstream across the basin, providing a sample of in situ measurements that was representative of concentrations across the entire basin for the first time.

We used the TOMCAT atmospheric model in order to simulate CO and CH_4 in the Amazon basin, before comparing these simulations to the new observations. Comparison of observed and simulated CO concentrations allowed us to revise downwards estimates of CO emissions (and therefore also CH_4 emissions) from fires within the basin during the biomass burning season (July – September). Using the Joint UK Land Environment Simulator (JULES) to provide wetland methane emissions estimates, comparing simulated and observed CH_4 concentrations (see Figure 1) allowed us to scale our initial emission estimates in order to minimise model-observation differences and provide optimised emission estimates for the region.

Key results and impacts

This study was the first time that long-term in-situ measurements, representative of concentrations from across the Amazon basin, were used in order to constrain estimates of surface fluxes of CH_4 from within the region. We found that previous biomass burning emissions of CO and CH_4 were significantly overestimated in 2010, whilst total CH_4 emissions were underestimated in both years. Our optimised estimates of 36.5–41.1 Tg(CH_4)/yr in 2010 and 31.6–38.8 Tg(CH_4)/yr in 2011 indicate that the basin contributed approximately 7% of global CH_4 emissions to the atmosphere.

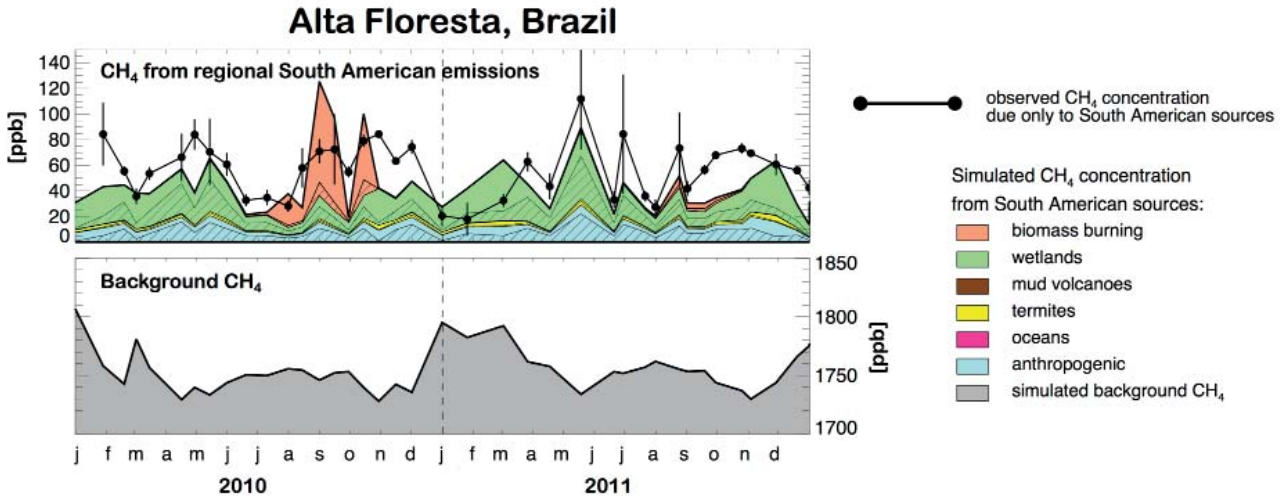

Figure 1. Observed and simulated CH_4 concentrations, with background CH_4 concentrations subtracted (ppb, top panel) in 2010 and 2011 at a measurement site located at Alta Floresta in the Amazon Basin. Also shown is the simulated background CH_4 concentrations (ppb, bottom panel). 'Background' represents CH_4 that has been transported into the basin from other regions of the globe (even if it had originally been emitted within the basin and then transported away). Observations are shown as black circles, with vertical black lines signifying 1σ of theobservations. Solid colour blocks represent simulated CH_4 emitted within South America, tagged according to emission type. Unhatched coloured sections indicate CH_4 emitted within the Basin, while hatched sections represent CH_4 emitted in non-Amazonian South America. The differences between the simulated and observed CH_4 concentrations allow us to scale the emissions used in the model in order to match the observed concentrations, providing an optimal estimate of total Amazon methane emissions.

Featured publication

Wilson, C., M. Gloor, L. V. Gatti, J. B. Miller, S. A. Monks, J. McNorton, A. A. Bloom, L. S. Basso, and M. P. Chipperfield (2016), Contribution of regional sources to atmospheric methane over the Amazon Basin in 2010 and 2011, *Global Biogeochem.* Cycles, 30, doi: 10.1002/2015GB005300.

GLOBAL RETRIEVALS OF THE TERRESTRIAL CARBON CYCLE

Jean-François Exbrayat and Mathew Williams, NCEO Edinburgh

The global terrestrial carbon cycle is poorly constrained because of limited understanding of key ecosystem states and functions, and the innate heterogeneity and dynamism of the land surface. Imposing observational constraints on ecosystem carbon models is therefore needed to improve our knowledge of the current state of the C cycle, and potentially improve our capacity to predict its future. Here we merge available observational datasets, including satellite data, with a state-of-the-art ecosystem model to generate constrained estimates of fluxes and stocks, but also maps of key process parameters, across the globe.

Methodology

We used the Carbon Data-Model Framework (CARDAMOM), a model-data fusion tool we have developed, to retrieve the global terrestrial carbon cycle for the period spanning 2001 to 2010. CARDAMOM applies a Bayesian Markov-Chain Monte-Carlo algorithm to an ecosystem model in order to retrieve the terrestrial carbon cycle in agreement with observations relevant to the biosphere while satisfying a large set of Ecological and Dynamic Constraints (Bloom and Williams, 2015).

For this study, the model-data fusion procedure was applied in more than 13,000 pixels at a 1°x1° spatial resolution, using ERA-Interim re-analysis climate data and MODIS burned area as drivers while assimilating time series of leaf area index, biomass, soil carbon content derived from satellite observations and global databases. The Bayesian approach provides explicit confidence intervals of parameters values and hence ecosystem carbon fluxes as well as carbon stocks increment through time. Unlike most terrestrial ecosystem models, CARDAMOM does not rely on pre-defined land cover types. This way, we are able to produce continuous maps of key ecosystem function properties in agreement with the aforementioned observational datasets.

Key results and impacts

Global relationships emerge in the spatial distribution of key ecosystem functioning properties that can be validated with in-situ trait observations. Allocation of primary productivity to structural carbon (wood and roots) is higher in the wet tropics than at higher latitudes, where plants allocate relatively more carbon to the photosynthetic parts. Live biomass and dead organic matter residence times do not correlate. We show that there is a mismatch between the spatial variability of our retrievals and current land cover maps. This has strong implications for the prediction of terrestrial carbon dynamics, which are currently based on globally applied parameters linked to land cover or plant functional types.

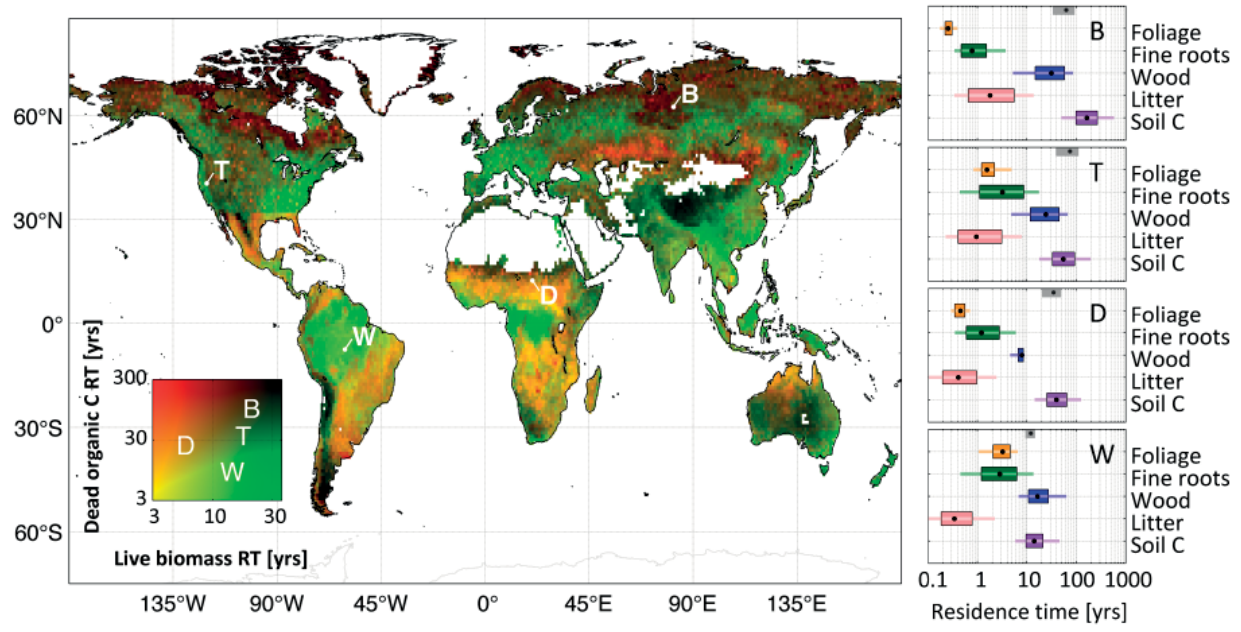

Figure 1. Retrievals of C residence time (RT) in live biomass and dead organic C pools; residence times are retrieved at 1° × 1° using a Bayesian MDF approach. Brown denotes ecosystems with high residence times for all C pools, green denotes ecosystems with long live biomass C residence times, and orange denotes ecosystems with low live biomass residence time. The residence times for individual C pools at locations B, T, D, and W are shown on the Right (black dot, median; box, 50% confidence range; line, 90% confidence range). Mean C residence times from Carvalhais et al. (2014) are shown as gray boxes (50% confidence intervals) and black dots (medians).

Featured publication

Bloom AA, Exbrayat J-F, van der Velde IR, Feng L, Williams M (2016) The decadal state of the terrestrial carbon cycle: global retrievals of terrestrial carbon allocation, pools and residence times. *Proceedings of the National Academy of Sciences* 113:1285–1290. doi: 10.1073/pnas.1515160113.

COMBINING SATELLITES AND ARGO-FLOATS TO QUANTIFY ENERGY SOURCES SUPPORTING LIFE IN THE DEEP, DARK OCEAN

Giorgio Dall'Olmo, Robert Brewin, NCEO and Plymouth Marine Laboratory

The part of the ocean between 100 m and 1000 m is called the mesopelagic region. This region contains one of the largest ecosystems on the planet and most of the ocean's fish. Yet the mesopelagic remains a vastly unexplored and poorly understood ecosystem. Basic questions such as what energy fuels the mesopelagic ecosystem, remain only partially answered. Up to now this ecosystem has been thought to be sustained by a 'rain' of fast-sinking organic aggregates of dead plankton and waste products from surface-living organisms – the so-called biological carbon pump. Whilst this source of organic carbon is very important, marine scientists have come to realize that it simply is not sufficient to support the vast numbers and variety of organisms that live in the mesopelagic layer, and have investigated another oceanographic mechanism – the seasonal mixed-layer pump. This pump takes non-sinking particles as well as dissolved organic carbon from surface waters into the depths, and thus supplies an additional pulse of organic carbon to the mesopelagic. During spring-time stormy conditions, strong winds mix surface water and the organic carbon it contains deep into the ocean. This deeply-mixed carbon is then 'trapped' inside the mesopelagic region when the shallow summer mixed layer forms and becomes available as an energy source to mesopelagic organisms. Overall, these variations in the surface mixed layer could thus pump part of the missing carbon into the mesopelagic, but there has never been a concerted effort to estimate the total flux of organic carbon that they supply across the world ocean.

Methodology

Now Plymouth Marine Laboratory (PML) scientists, funded via the UK National Centre for Earth Observation, working with colleagues from France, have estimated this amount. By combining satellite data from the European Space Agency Ocean Colour-Climate Change Initiative with in-situ measurements obtained by Argo and new Bio-Argo floats, partially-funded by the UK Natural Environment Research Council, they estimate that the pump moves around 300 million tons of carbon each year. In the deeply-mixed high-latitude regions, the figure represents an average of 23%, but possibly in excess of 100% of the better studied flux of faster-sinking, larger particles and aggregates.

Key results and impacts

Most methods for measuring carbon transport into the deep ocean have concentrated on the particles that sink at relatively fast rates, but have not measured how neutrally-buoyant or slowly-sinking organic particles are redistributed through the water column. This means that current global estimates of carbon export in the ocean are missing the potentially important contribution from the seasonal mixed-layer pump. Our new global estimates should thus be considered as an additional flux of organic carbon to the mesopelagic region that was previously not accounted for, and that's important when we try to understand which sources of energy fuel the mesopelagic ecosystem.

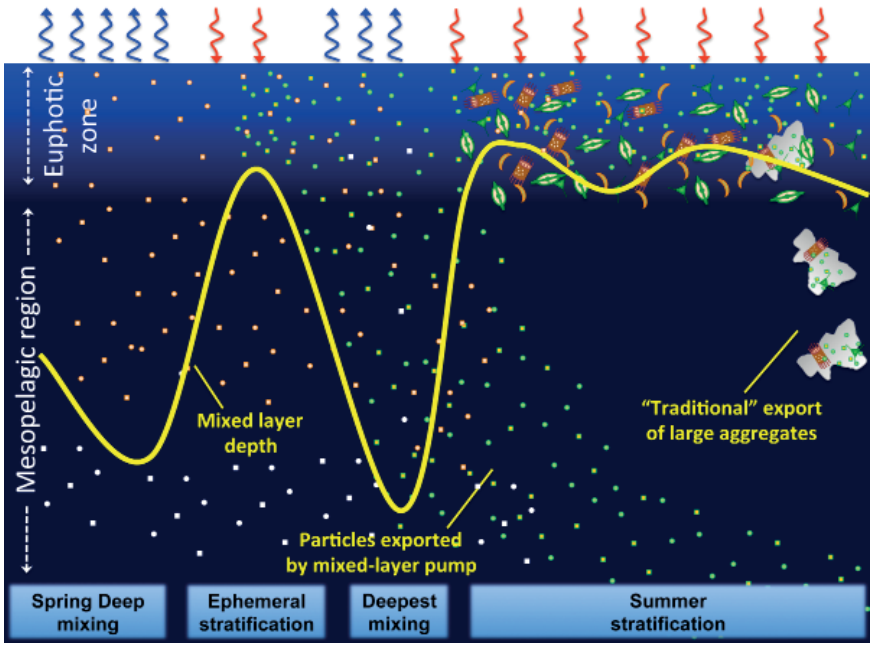

Figure 1. Schematic demonstrating how seasonal variations in mixed-layer depth can pump organic particles from the surface to the mesopelagic ecosystem.

Featured publication

Giorgio Dall'Olmo, James Dingle, Luca Polimene, Robert J. W. Brewin& Hervé Claustre, Substantial energy input to the mesopelagic ecosystem from the seasonal mixed-layer pump, *Nature Geoscience* (2016), doi: 10.1038/ngeo2818.

Additional science references

Bloom AA, Williams M (2015) Constraining ecosystem carbon dynamics in a data-limited world: integrating ecological "common sense" in a model–data fusion framework. *Biogeosciences* 12:129–1315. doi: 10.5194/bg-12-1299-2015.

Carvalhais N, et al. (2014) Global covariation of carbon turnover times with climate in terrestrial ecosystems. *Nature* 514:213–217. doi: 10.1038/nature13731.

BIOMASS BURNING EMISSION RATIOS DERIVED FROM SATELLITE OBSERVATIONS OF THE 2015 INDONESIAN FIRE PLUMES

Rob Parker, Hartmut Boesch, David Moore, NCEO Leicester; and Martin Wooster, NCEO King's College London

Through collaboration with NCEO and international colleagues and as part of Robert Parker's ESA Living Planet Fellowship (ELEGANCE-GHG), we have developed the capability to determine the emission ratio of atmospheric carbon dioxide and methane released during intensive biomass burning events, such as the one in Indonesia related to the 2015/2016 El Niño event. This builds on work we first published in Ross et al., 2013.

Methodology

The 2015/2016 El Niño event had a dramatic impact on the amount of Indonesian biomass burning and subsequent greenhouse gas emission. Satellite observations of CH_4 and CO_2 from the GOSAT satellite produced for the ESA GHG-CCI project (Parker et al., 2015) were used to probe aspects of the chemical composition of these fires, with large enhancements observed due to the fire emissions.

By careful selection of measurements representing background conditions, excess concentrations directly related to the fires were inferred from the satellite data and from these excess concentrations, emission ratios of CH_4/CO_2 were calculated (Figure 1). An emission ratio of 6.2 ppb/ppm was derived for the Indonesian region, indicative of smouldering combustion, consistent with the primary fuel source being peatland (Figure 2). The same methodology was applied to Southern Africa where an emission ratio of 4.3 ppb/ppm was found, consistent with the flaming combustion of savannah/grasslands that typify the region and have previously been confirmed via local in-situ measurements. Finally, the emission ratio over the Amazon region was calculated to be 5.1 ppb/ppm, again consistent with the known fuel type for this region which leads to a combination of smouldering and flaming burning.

Key results and impacts

The ability to determine large-scale ERs from satellite data allows the combustion behaviour of very large regions of burning to be characterised and understood in a way not possible with ground-based studies, and which can be logistically difficult and very costly to consider using aircraft observations. We therefore believe the method demonstrated here provides an important tool for characterising biomass burning emissions, and that the GHG ERs derived for the first time for these large-scale Indonesian fire plumes during an El Niño event point to more routinely assessing spatiotemporal variations in biomass burning ERs using future satellite missions.

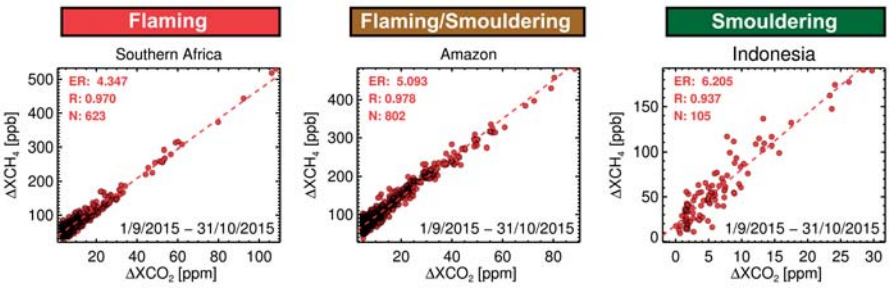

Figure 1. Scatterplots showing the satellite-derived excess concentrations of CH_4 and CO_2. The gradient of the fit gives the derived emission ratio (ER). An ER > 6 suggests that the fire behaviour is dominated by smouldering combustion, with < 4.5 typical of flaming combustion. Values in between suggest a combination of both types. Analysis over Indonesia, Southern Africa and the Amazon calculated ERs consistent with the known fuel types in these regions and agree closely to measurements made in-situ by ground-based instrumentation.

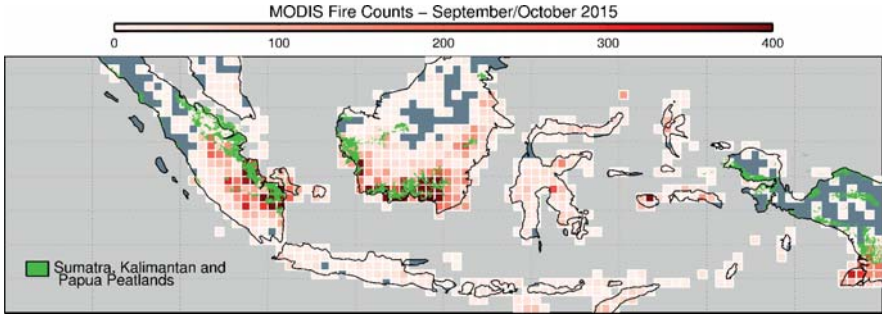

Figure 2. Satellite fire counts for September–October 2015 over Indonesia, gridded into 0.5°x0.5° boxes. Also overlaid are the locations of known peatlands in Sumatra (left), Kalimantan (centre) and Papua (right) showing that the fire activity was primarily located in areas dominated by peatlands.

Featured publication

Parker, R. J. et al. (2016): Atmospheric CH_4 and CO_2 enhancements and biomass burning emission ratios derived from satellite observations of the 2015 Indonesian fire plumes, *Atmos. Chem. Phys.*, 16, 10111–10131, doi: 10.5194/acp-16-10111-2016.

Additional science references

Ross, A. N., M. J. Wooster, H. Boesch, and R. Parker (2013), First satellite measurements of carbon dioxide and methane emission ratios in wildfire plumes, *Geophys. Res. Lett.*, 40, 4098–4102, doi: 10.1002/grl.50733.

Parker, R. J., Boesch, H., Byckling, K., Webb, A. J., Palmer, P. I., Feng, L., Bergamaschi, P., Chevallier, F., Notholt, J., Deutscher, N., Warneke, T., Hase, F., Sussmann, R., Kawakami, S., Kivi, R., Griffith, D. W. T., and Velazco, V. (2015): Assessing 5 years of GOSAT Proxy XCH_4 data and associated uncertainties, *Atmos. Meas. Tech.*, 8, 4785–4801, doi:10.5194/amt-8-4785-2015.

QUANTIFYING FOREST BIOMASS STOCKS IN MEXICO USING SAR, OPTICAL AND TOPOGRAPHIC DATASETS

Pedro Rodriguez-Veiga and Heiko Balzter, NCEO Leicester

Mexico's forests cover 65 million ha of land area. Accurate reporting of their aboveground biomass (AGB) is a requirement of international policies to mitigate climate change through the reduction of greenhouse gas emissions from deforestation and forest degradation, as well as the enhancement of existing forest carbon stocks (REDD+ initiative). Existing forest biomass maps show discrepancies with forest inventory observations in Mexico (Rodriguez-Veiga et al., 2016). A probabilistic method based on the Maximum Entropy (MaxEnt) algorithm improves satellite estimates by combining different sensors and characterizes the uncertainty at pixel level.

Methodology

National forest inventory data (INFyS) were used to calibrate a MaxEnt algorithm to generate probability distribution functions of forest biomass (AGB) per pixel (Rodriguez-Veiga et al., 2016). Those were used to produce a national forest biomass map (Figure 1), its spatially explicit uncertainty, and maps of the probability of the pixel being forest, at 250 m spatial resolution. The input predictor layers were extracted from the Moderate Resolution Imaging Spectrometer (MODIS), ALOS PALSAR Lband dual-polarization Synthetic Aperture Radar (SAR), and the Shuttle Radar Topography Mission (SRTM) digital elevation model. Jackknife analysis of the model accuracy indicated that SAR made the greatest contribution to the biomass estimation (50.9%), followed by the optical sensor (32.9%) and the terrain elevation from SRTM (16.2%) (Figure 2). Different forest masks based on the same forest definition but generated using different sensors were also used to produce estimates of carbon stocks for Mexico.

Key results and impacts

The forest biomass map showed a root mean square error of 17.3 t C ha^{1}. The use of different forest cover masks yielded large differences of about 30 million ha in forest cover extent and 0.45 Gt C in total carbon stocks. We estimate the total carbon stored in the forest biomass of Mexico as 1.69 Gt C ± 1%, in broad agreement with the Food and Agriculture Organisation (FAO) Forest Resources Assessment 2010 (1.68 Gt C). The new biomass map, derived directly from the biomass estimates of the national forest inventory and the satellite data, has similar overall accuracy to previous forest biomass maps of Mexico, but crucially, it is more representative of the shape of the probability distribution function of biomass in the national forest inventory data. Our results suggest that the use of a non-parametric Maximum Entropy model trained with forest inventory plots, even at the sub-pixel size, can provide accurate spatial maps for national or regional REDD+ Monitoring, Reporting and Verification (MRV) activities.

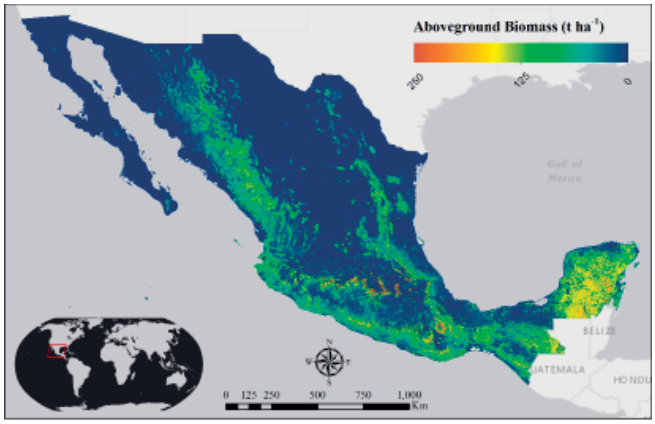

Figure 1. Aboveground forest biomass map for Mexico at 250 m spatial resolution for 2008.

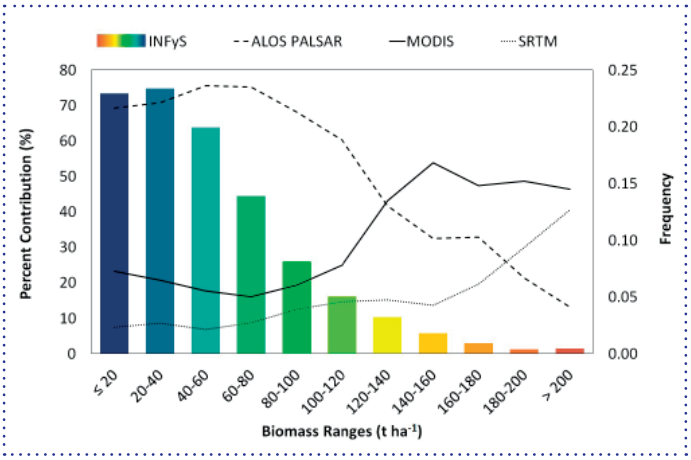

Figure 2. Percent contribution of each spatial dataset to the AGB map per biomass range (lines) and frequency AGB from the INFyS ground plots (coloured columns)

Featured publication

Rodriguez-Veiga, P., Saatchi, S., Tansey, K. & Balzter, H. 2016. Magnitude, spatial distribution and uncertainty of forest biomass stocks in Mexico. *Remote Sensing of Environment*, 183, 265–281, http://dx.doi.org/10.1016/j.rse.2016.06.004, ISSN: 0034-4257*.

* This research was also supported by the EC project GIONET (Grant Agreement PITN-GA-2010-264509), and the ESA GlobBiomass project (ESRIN contract no. 4000113100/14/I-NB).

ESTIMATING LANDSCAPE FIRE EMISSIONS FROM FIRE RADIATIVE POWER AND APPLICATION TO MARITIME SOUTHEAST ASIA IN 2015

Martin Wooster, Daniel Fisher, Weidong Xu, Jiangping He, NCEO King's College London

There has been continued development of fire radiative power (FRP) products from different Earth Observing systems, including both polar orbiting and geostationary systems (e.g. Wooster et al., 2015). We are now seeing a strong uptake of this FRP data in both science papers and operational applications. And example of both is provided by the Copernicus Atmosphere Monitoring Service (CAMS), where the integral Global Fire Assimilation System (GFAS) uses FRP data to produce daily global fire emission estimates. Recently the CAMS system has been used for a science study where, in conjunction with *in situ* and EO-derived observations of the fire-emitted smoke, it was used to generate regional estimates of greenhouse and reactive gases over maritime southeast Asia for the extreme, El Niño driven wildfires of September and October 2015, where we estimate that 227 ± 67 Tg of carbon was released into the atmosphere.

Methodology

To determine fire carbon emissions an approach combining in-situ observations with EO constrained atmospheric model outputs was used. The field measurement campaign captured snapshots of the landscape fire emissions that enabled the derivation of emission factors and their ratios linking amounts of emitted CO to those of CO_2 and CH_4 for the first time in SE Asian peatland fires. These three trace gases typically comprise >95% of C released during biomass burning events, so are the key to estimating total fire carbon emissions. Regional CO emission estimates were derived with the modelling and assimilation framework of CAMS, which includes assimilation of EO derived landscape burning FRP estimates. The CO emission estimates from CAMS were constrained by matching model estimates of CO atmospheric distribution to total atmospheric CO column amounts derived from the Measurements of Pollution in the Troposphere (MOPITT) instrument. Total regional biomass burning C emission for the fire events was then inferred through application of the aforementioned emission factor ratios for CO_2 and CH_4 to the regionally optimised CO emissions estimates.

Key results and impacts

The total carbon released by the fires for the period September to October 2015 was 227 ± 67 Tg C, of which 83% was in the form of CO_2 (692 Tg), 16% in the form of CO (84 Tg), and 1% in the form of CH_4 (3.2 Tg), and these carbon emissions from the 2015 fires are the largest seen in maritime southeast Asia since those associated with the record breaking El Niño of 1997. This is more carbon than the entire European Union emitted to the atmosphere in the same period from all industrial and automotive sources, and led to a maximum of contribution of 0.14 ppm to the anomalously high global CO_2 growth rate observed in 2015 (the largest every recorded). Most of the released carbon, given its 'fossil carbon' source in the form of peat, constitutes a permanent addition of CO_2 to the atmosphere rather than one that will be re-assimilated by vegetation regrowth.

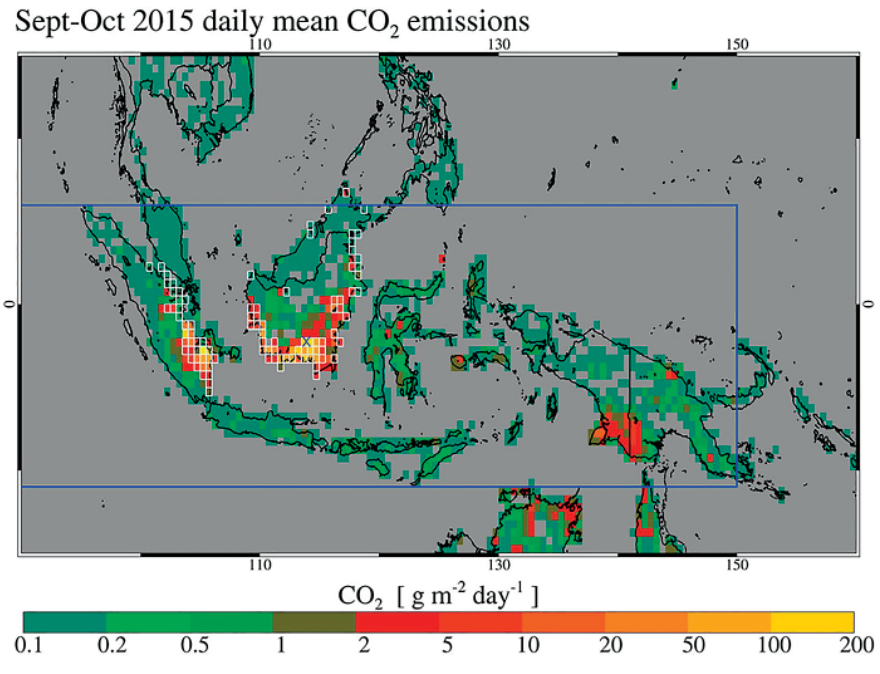

Figure 1. Daily mean CO_2 emissions from peat and vegetation fires burning across maritime southeast Asia in Sept-Oct 2015, presented in 0.5° × 0.5° grid cells.

Featured publication

Huijnen, V., Wooster, M.J., Kaiser, J.W., Gaveau, D.L.A., Flemming, J., Parrington, M., Inness, A., Murdiyarso, D., Main, B. and van Weele, M., 2016. Fire carbon emissions over maritime southeast Asia in 2015 largest since 1997. *Scientific reports*, 6, p.26886. doi: 10.1038/srep26886.

Additional science references

Wooster, M. J., Roberts, G., Freeborn, P. H., Xu, W., Govaerts, Y., Beeby, R., He, J., Lattanzio, A., Fisher, D., and Mullen, R.: LSA SAF Meteosat FRP products – Part 1: Algorithms, product contents, and analysis, *Atmos. Chem. Phys.*, 15, 13217–13239, doi:10.5194/acp-15-13217-2015, 2015.

Roberts, G., Wooster, M. J., Xu, W., Freeborn, P. H., Morcrette, J.-J., Jones, L., Benedetti, A., Jiangping, H., Fisher, D., and Kaiser, J. W.: LSA SAF Meteosat FRP products – Part 2: Evaluation and demonstration for use in the Copernicus Atmosphere Monitoring Service (CAMS), *Atmos. Chem. Phys.*, 15, 13241–13267, doi:10.5194/acp-15-13241-2015, 2015.

CONSISTENT REGIONAL FLUXES OF CH_4 AND CO_2 INFERRED FROM GOSAT PROXY XCH_4:XCO_2 RETRIEVALS, 2010–2014

Liang Feng, Paul Palmer, NCEO Edinburgh, and Hartmut Boesch, Robert Parker, NCEO Leicester

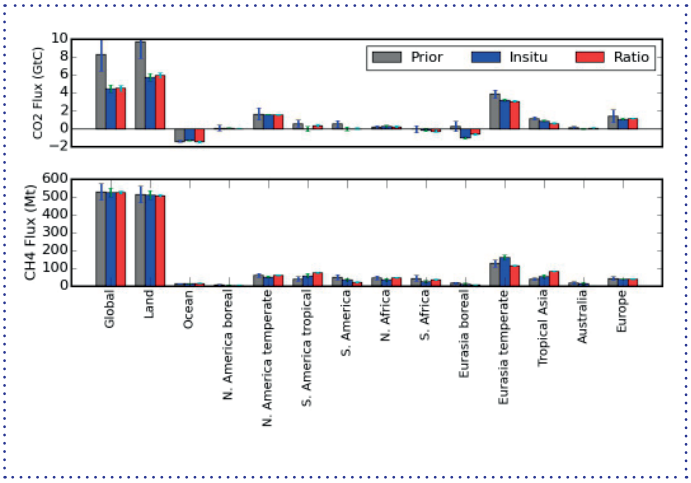

Figure 1. Annual mean (2010-2014, inclusive) regional net fluxes of (top) CO_2 and (bottom) CH_4 fluxes inferred from the (red) ratio experiments and the (green) in situ experiments. The grey columns represent the a priori estimates and the vertical lines superimposed on these columns denote the one-sigma error.

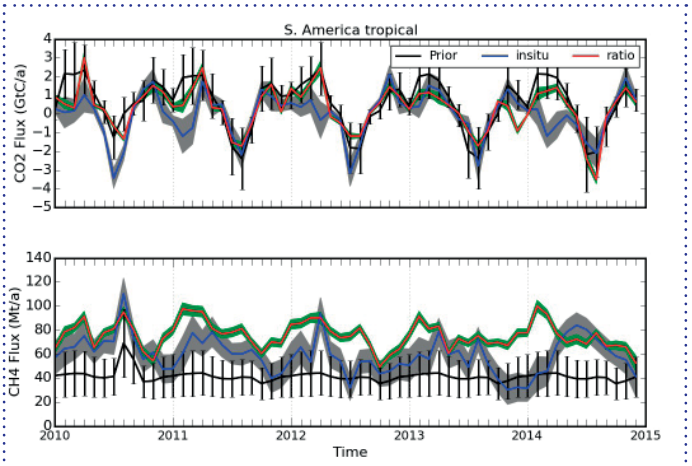

Figure 2. The net monthly net CO_2 and CH_4 fluxes over tropical South America inferred from (red) GOSAT data are compared with the (black) a priori, and fluxes inferred from using only (blue) in situ data only. The vertical lines (envelopes) represent the a priori (a posteriori) uncertainties.

We present the first multi-year record of self-consistent regional net fluxes (sources minus sinks) of CO_2 and CH_4 inferred from the Japanese Greenhouse gases Observing SATellite (GOSAT). These fluxes are inferred from GOSAT XCH_4:XCO_2 retrievals, which are less prone to systematic errors than XCO_2 or XCH_4 retrievals. Our large-scale results are consistent with in situ data, but with smaller uncertainties. We find evidence that the carbon balance of tropical South America was perturbed following the droughts of 2010 and 2012, with net annual fluxes not returning to an approximate annual balance until 2013. We find no evidence that these droughts affected continental-scale CH_4 fluxes.

Methodology

One implication of the atmospheric growth of CO_2 and CH_4 is an increase in global mean temperatures. The most recent international climate agreement aims to limit the rise in global mean temperature to 2 degrees Celsius, which will be attempted by reducing the emissions of human-driven GHGs. The Japanese satellite GOSAT is purposely designed to measure atmospheric CO_2 and CH_4 columns at an unprecedented precision to improve our current estimates of surface GHG fluxes. However the flux estimates inferred from the GOSAT XCO2 or XCH4 retrievals are often found to be inconsistent with the results based on the surface network (particularly for CO_2), partly due to observation bias and varying coverage.

We build on previous NCEO-funded work that developed a novel approach to estimate simultaneously regional CO_2 and CH_4 flux estimates from the GOSAT XCH4:XCO2 ratio measurements (Fraser et al., 2014). We use an Ensemble Kalman Filter to assimilate the ratio data (produced by the University of Leicester, Parker et al., 2015) from January 2009 to December 2014, inclusive. We use individual in situ and GOSAT observations to estimate monthly fluxes at a higher spatial resolution than previous work.

Key results and impacts

The annual net a posteriori CO_2 fluxes inferred from GOSAT data are similar to those inferred from the in situ data but with smaller uncertainties, particularly over the tropics (Figure 1). But the CH4 fluxes inferred from GOSAT data show much higher emission from tropical lands, and much less emissions from extratropical regions.

Using GOSAT data we find that that the carbon balance of tropical South America was perturbed following the droughts of 2010 and 2012 with net annual fluxes not returning to an approximate annual balance until 2013 (Figure 2). These two large-scale Amazon droughts do not appear to affect the CH_4 fluxes.

Featured publication

Feng, L., Palmer, P. I., Bösch, H., Parker, R. J., Webb, A. J., Correia, C. S. C., Deutscher, N. M., Domingues, L. G., Feist, D. G., Gatti, L. V., Gloor, E., Hase, F., Kivi, R., Liu, Y., Miller, J. B., Morino, I., Sussmann, R., Strong, K., Uchino, O., Wang, J., and Zahn, A.: Consistent regional fluxes of CH4 and CO2 inferred from GOSAT proxy XCH4:XCO2 retrievals, 2010–2014, *Atmos. Chem. Phys. Discuss.*, doi: 10.5194/acp-2016-868, 2016.

Additional science references

Fraser, A., Palmer, P. I., Feng, L., Bösch, H., Parker, R., Dlugokencky, E. J., Krummel, P. B., and Langenfelds, R. L.: Estimating regional fluxes of CO_2 and CH_4 using space-borne observations of XCH_4: XCO_2, *Atmos. Chem. Phys.*, 14, 12883–12895, doi:10.5194/acp-14-12883-2014, 2014.

Parker, R. J., Boesch, H., Byckling, K., Webb, A. J., Palmer, P. I., Feng, L., Bergamaschi, P., Chevallier, F., Notholt, J., Deutscher, N., Warneke, T., Hase, F., Sussmann, R., Kawakami, S., Kivi, R., Griffith, D. W. T., and Velazco, V.: Assessing 5 years of GOSAT Proxy XCH_4 data and associated uncertainties, *Atmos. Meas. Tech.*, 8, 4785–4801, doi:10.5194/amt-8-4785-2015, 2015.

RAINFALL PATTERNS LINKED WITH ENERGY FLOW ACROSS EQUATOR

Richard Allan, NCEO Reading

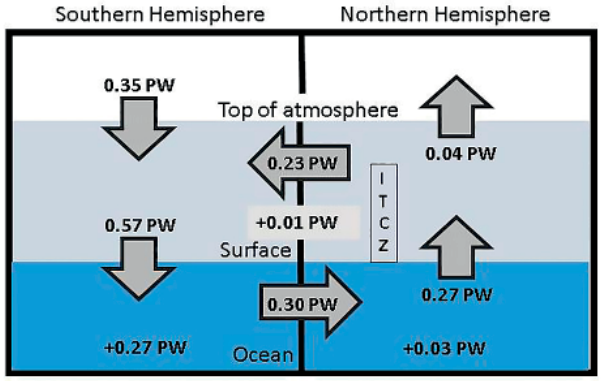

Figure 1. Schematic showing new observations of energy flows (arrows) in the climate system at the top of the atmosphere, at the surface and between northern and southern hemispheres in petawatts (PW: millions of billions of Joules per second of energy flux) and the location of the Inter Tropical Convergence Zone (ITCZ). Numbers without arrows denote accumulating energy in the atmosphere and ocean [more details at http://blogs.reading.ac.uk/weather-and-climate-at-reading/2016/energy-flows-rainfall-patterns-and-climate/].

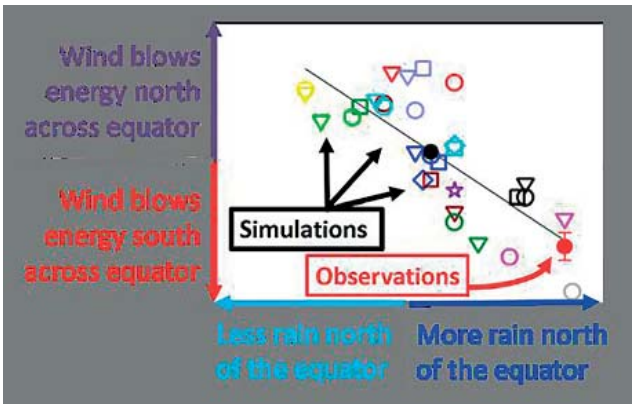

Figure 2. A schematic showing simulations (open symbols) that produce a northward flow of energy across the equator produce less rainfall north of the equator than south of the equator which disagrees with observations (filled red circle) [for more details, see Loeb et al. (2015), Figure 7d].

There is currently more sunlight absorbed by the Earth than is emitted as infrared energy to space. This energy "imbalance" is primarily explained by human-caused greenhouse gas emissions which are causing the planet to heat up. Combining satellite data with ocean measurements, we find that 300 million million Joules per second of energy is accumulating, much of it in the southern oceans. We calculated energy flows across the equator and discovered that climate simulations producing unrealistic northward flows of energy across the equator display inaccurate rainfall patterns. Our findings suggest that by improving simulated energy flows across the equator we may be able to predict rainfall patterns more accurately.

Methodology

In collaboration with NASA and the UK NERC DEEP-C project, satellite records of changes in the incoming and reflected sunlight and outgoing infrared radiative energy emitted to space were compiled. These were combined with reanalysis of the Earth's atmosphere (a combination of simulations and observations) and sub-surface ocean temperature records to calculate the flows of energy into and out of the top of the atmosphere, within the atmosphere and into and out of the Earth's surface. The satellite data provide detailed coverage and accurate changes in energy while these are anchored to a reliable rate of heat accumulation set by the ocean observations. Combining with atmospheric reanalyses we were able to compute energy flows between northern and southern hemisphere and into the southern and northern ocean surface. An updated estimate of these energy flows (in petawatts or million billion Joules per second, Figure 1) shows a build-up of heat due to human caused greenhouse gas emissions and that this is primarily entering the southern ocean. Our calculations show that the atmosphere moves around 0.23 petawatts of energy from the northern to southern hemisphere.

Key results and impacts

Our observed estimates of energy flows indicate that many computer simulations used to make future climate change projections are inaccurate. Climate simulations with the wrong direction of energy transport across the equator by atmospheric winds also have inaccurate rainfall patterns (See Figure 2). This has important implications for the reliability climate simulations in projecting future changes in rainfall patterns and further scrutiny of energy flows is warranted. This work has been discussed on a variety of blogs and publications and is relevant for the Intergovernmental Panel on Climate Change and policy makers interested in the reliability of climate simulations and their projected changes in rainfall patterns.

Featured publication

Featured publication: Loeb, N.G., H. Wang, A. Cheng, S. Kato, J.T. Fasullo, K.-M. Xu and R.P. Allan(2016) Observational Constraints on Atmospheric and Oceanic Cross-Equatorial Heat Transports: Revisiting the Precipitation Asymmetry Problem in Climate Models, *Climate Dynamics*, 46, 3239–3257, doi: 10.1007/s00382-015-2766-z

Additional science references

Liu, C. Allan, R. P., P. Berrisford , M. Mayer , P. Hyder, N. Loeb , D. Smith , P.-L. Vidale, J. Edwards (2015) Combining satellite observations and reanalysis energy transports to estimate global net surface energy fluxes 1985-2012, *J. Geophysical Research*, 120, 9374–9389, doi: 10.1002/2015JD023264.

Blog: http://blogs.reading.ac.uk/weather-and-climate-at-reading/2016/energy-flows-rainfall-patterns-and-climate/.

Blog: https://earthdata.nasa.gov/user-resources/sensing-our-planet/missing-heat.

Highlight: https://ncas.ac.uk/index.php/en/climate-science-highlights/2344-rainfall-patterns-linked-with-energy-flow-across-equator.

DETECTING MULTIDECADAL CHANGES IN THE EARTH'S OUTGOING LONGWAVE RADIATION SPECTRUM

Richard Bantges and Helen Brindley, NCEO Imperial College London

Measurements of the Earth's outgoing longwave radiation (OLR) spectrum provide a means to identify and monitor the effects of many different key climate processes. With observations now spanning more than four decades, differences between the Earth's global mean OLR spectrum as observed from satellite instruments flying in 1970, 1997 and 2012 were calculated. These differences were examined, in conjunction with reanalyses data, to determine whether they could be used to discern robust signatures of the climate response to increasing greenhouse gases over the period in question. We find that uncertainties in the calibration of the earliest instrument preclude the use of these data for the quantitative assessment of forcing and feedback processes.

Methodology

Data from the Interferometric Infrared Sounder (IRIS) in 1970, followed by the Interferometric Monitor for Greenhouse Gases (IMG) in 1997 and finally the Infrared Atmospheric Sounding Instrument (IASI) in 2012, were compared. Owing to the different characteristics of each instrument, obtaining meaningful comparisons required each data set to be processed to produce data at the same spectral resolution, over a common wavenumber range and at a similar spatial resolution. To avoid seasonal artefacts, only data from April to June for each year were retained. The OLR radiance data for the three years were then averaged into three-month, area weighted global averages and converted into equivalent brightness temperature (T_B) spectra, and the differences between the years calculated. To investigate the robustness of the differences observed, matched, simulated spectra for the equivalent periods were generated by effectively flying each satellite through ECMWF reanalyses data sets. Observed spectral differences relative to IRIS, in combination with the simulations, indicated a potential issue with the IRIS calibration (Figure 1). This was further confirmed by probability density functions of the T_B differences between 909cm^{-1} and 1250cm^{-1} (Figure 2).

Key results and impacts

In a warming scenario, in the absence of a compensating change in cloud properties, one would expect to see an increase in global mean brightness temperatures within the atmospheric window (750–1000 and 1080–1200 cm^{-1}). Figure 1 shows such an increase but it is somewhat larger than would be expected given decadal trends in surface temperature and shows a distinct 'break' across the 1042 cm^{-1} ozone band. A similar differential signature is not seen in the reanalyses. Figure 2 suggests that this signal is related to the temperature of the scene observed by IRIS. The study reiterates the need for high accuracy, SI traceable measurements of the Earth's outgoing radiance spectra if one is to have confidence in the signals of change as measured by different instruments, especially those separated in time.

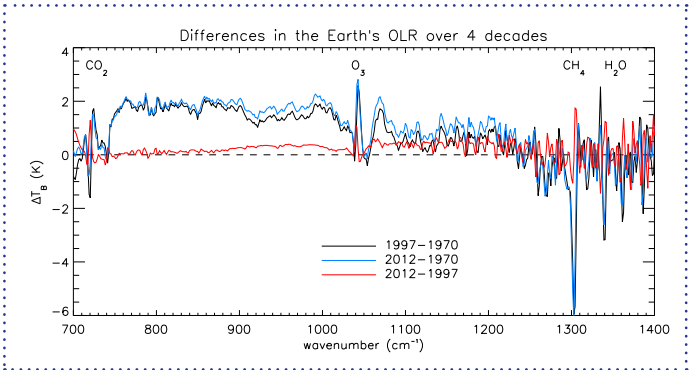

Figure 1. Differences, shown in equivalent brightness temperature, in the Earth's OLR radiated to space derived from 3-month averaged satellite observation records from 1970, 1997 and 2012. Noticeable features include those in the labelled CO_2, O_3, CH_4 and H_2O bands, with a surprisingly large change in the two window regions (750 to 1000 cm^{-1} and 1050 to 1250cm^{-1}) either side of the O_3 band for differences from 1970.

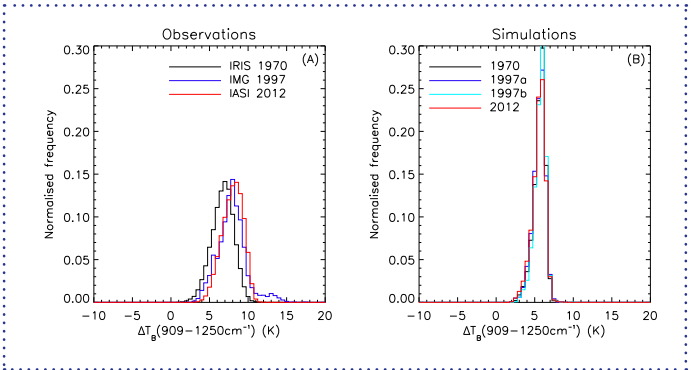

Figure 2. Normalised distributions contrasting the frequency and magnitude of the step-change in OLR across the two window regions (see figure 1) for the three different years; (A) for the observations, (B) for the simulations using ECMWF reanalyses data sets. The IRIS observations from 1970 appear to be shifted, something not seen in the simulations.

Featured publication

Bantges, R.J. et al., 2016: On the Detection of Robust Multidecadal Changes in Earth's Outgoing Longwave Radiation Spectrum, J. *Climate*, doi: 10.1175/JCLI-D-15-0713.1.

Acknowledgements

Simulations were performed by X.H. Chen and X. L. Huang at the University of Michigan (USA).

MICRO-PHYSICAL STRUCTURE OF DEEP CONVECTIVE CORES

Alessandro Battaglia, NCEO Leicester

Due to the large natural variability of its micro-physical properties, the characterization of solid precipitation is a longstanding problem. Since in situ observations are unavailable in severe convective systems, innovative remote sensing observations are paramount to extend our understanding of such systems.

Methodology

Our group at the University of Leicester has developed a micro-physics retrieval technique based on an optimal estimation approach able to estimate the density, mass, and effective diameter of graupel and hail in severe convection through the combination of microwave multi-frequency active and passive airborne observations. The algorithm has been applied to study two convective cells that developed in North Carolina on the 23rd May during the IPHEx/RADEx14 campaign.

The NASA ER-2 plane observations consist of radiometric data, in the frequency bands between 10 and 85 GHz, and radar measurements at 9.6, 13.9, 35.3 and 94 GHz. The X-band radar data associated with this event is presented in Figure 1. The retrieved mean mass diameter of ice particles compares well with the polarimetric hydrometeor classification based on the ground-based S-band measurements (Figure 2), but additionally mass and density of ice species is estimated. Unequivocally the two cells contained very large density ice as confirmed by ground reports.

Key results and impacts

This work confirms that in deep convective systems air-borne radar measurements are the result of interplay between attenuation, Mie and multiple scattering effects, with the high frequency observations affected the most. It has been shown that in the core of convection, where high density ice particles might be present, the significant part of measured radiation comes from multiply scattered signal aloft. This has strong implications for satellite rainfall retrievals, which by not accounting for this phenomenon, tend to bias the rain rate in extreme weather conditions.

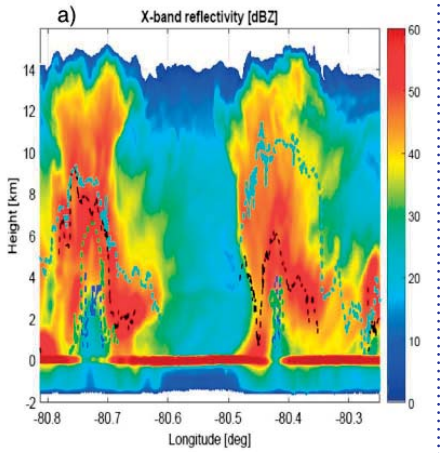

Figure 1. The reflectivity profiles measured by the ER-2 X-band radar on 23 May 2014 in correspondence to the thunderstorm occurred in North Carolina, during IPHEx/RADEx14 joint campaign. The blue, green, black and cyan lines correspond to the level below which the multiple scattering contribution becomes predominant at X, Ku, Ka, and W, respectively. Two regions of strong attenuation (80.43°W and 80.73°W) are associated with heavy rainfall whereas the neighbouring areas where high reflectivity values are observed (80.47°W and 80.76°W) correspond to the presence of two hail shafts (see Fig. 2).

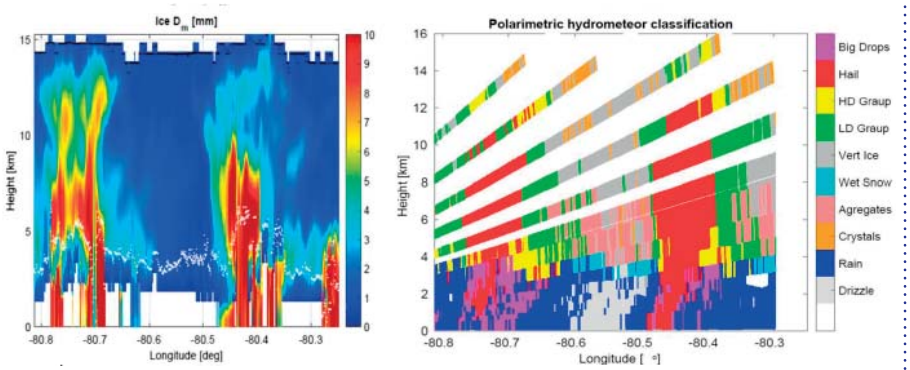

Figure 2. The retrieval of the mass-weighted mean volume diameter corresponding to the convective cells from Figure 1 and the hydrometeor classification reconstructed from the ground-based S-band radar for the same scene. The mass estimate is one of the output of the micro-physical retrieval developed in Leicester. It is based on the optimal estimation technique and utilizes measurements from active and passive instruments on-board the ER-2 plane. There is a clear correspondence between regions where the large diameter of hydrometeors is retrieved and the high density ice shafts highlighted by the ground-based algorithm, especially above the freezing level where attenuation effects are less significant.

Featured publication

Battaglia, A., K. Mroz, T. Lang, F. Tridon, S. Tanelli, L. Tian, and G. M. Heymsfield (2016), Using a multiwavelength suite of microwave instruments to investigate the microphysical structure of deep convective cores, *J. Geophys. Res. Atmos.*, 121, 9356–9381, doi: 10.1002/2016JD025269

Additional science references

Battaglia, A., S. Tanelli, K. Mroz, and F. Tridon, (2015): Multiple scattering in observations of the GPM dual-frequency precipitation radar: evidence and impact on retrievals. *J. Geophys. Res.*, 10.1002/2014JD022866

Battaglia, A., K. Mroz, F. Tridon, S. Tanelli, P.-E. Kirstetter, (2016). Multiple-scattering-induced "ghost echoes" in GPM-DPR observations of a tornadic supercell. *J. Appl. Meteor.* Climatol. http://journals.ametsoc.org/doi/ref/10.1175/JAMC-D-15-0136.1

Phil Harris, Christopher Taylor NCEO and Centre for Ecology & Hydrology; Belen Gallego-Elvira, Centre for Ecology & Hydrology; Darren Ghent, NCEO Leicester

GLOBAL DIAGNOSIS OF SOIL MOISTURE CONTROL ON THE LAND SURFACE FLUX PARTITION

Soil moisture plays a central role in the partition of net radiation at the land surface into sensible and latent heat flux. However, our understanding of where in the world this partition is constrained by soil moisture has been hindered by a lack of large-scale observations. Through NCEO and NERC-funded research, we have developed a new method to diagnose this constraint using satellite observations of rainfall and land surface temperature (LST) during rain-free dry spells. This is achieved by calculating how rapidly the land warms relative to the overlying atmosphere during these dry periods. Crucially, the variation in these warming rates with antecedent rainfall identifies different evaporation regimes.

Methodology

As the land surface dries during rain-free periods, evaporation may decrease due to a lack of soil moisture. In this case, energy normally used for evaporation is used to directly heat the atmosphere, a process that is accompanied by an increase in LST. To characterise this behaviour, dry spell events for the years 2000 to 2014 were identified using a combination of three satellite precipitation products (TRMM, CMORPH and PERSIANN) at 0.5° resolution. We focused on dry spells of 10 days or more during which daytime air temperature remained above 10°C.

Within these events, we analysed LST from MODIS Terra and Aqua, and reanalysis air temperature from ERA Interim. Anomalies in LST were calculated from the 1 km MODIS observations and then averaged across 1000s of dry spell events to reveal the typical surface behaviour. Specifically, we determined how rapidly on average the surface warms relative to the near-surface air to yield a Relative Warming Rate (RWR). Additionally, in order to distinguish the behaviours of different land cover types within the large-scale grid boxes, the 1 km LST were analysed separately for three broad categories (forest, grassland and bare ground) and RWR calculated for each one.

Key results and impacts

The results showed that 73% of the land surface between 60°S and 60°N warms faster than the atmosphere (Fig. 1a), indicating increases in sensible heat flux due to water-stressed conditions. Higher RWRs were found for short vegetation and bare ground than for tall, deep-rooted vegetation (Fig. 1b–d), due to differences in both the aerodynamic and the hydrological properties of those surfaces. This study provides the first global scale observational analysis of how the surface energy partition changes as soils dry. This method provides valuable new tools to evaluate the role of soil moisture in Earth System Models using the well-established satellite observations of LST.

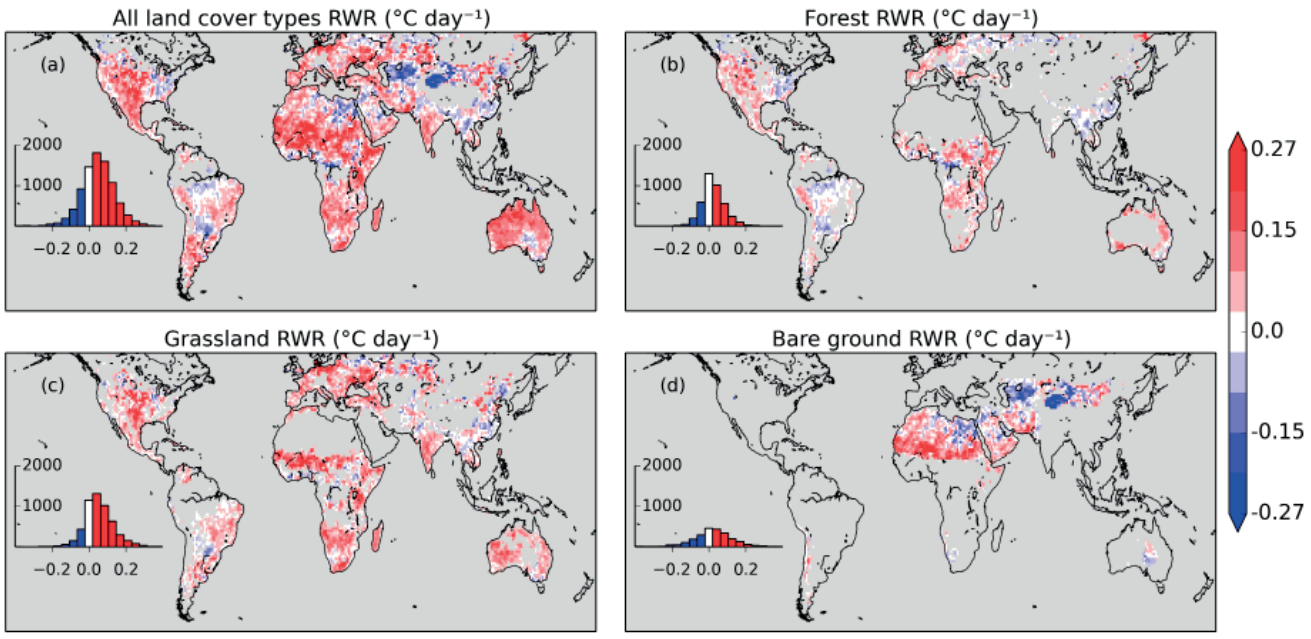

Figure 1. Relative land surface warming rates (RWRs) calculated from MODIS land surface temperature (LST) and ERA-Interim air temperature data during 10-day dry spells. The data in (a) represent all land cover types, whilst the analysis in restricted in the remaining plots to (b) forest only, (c) grassland only and (d) bare ground only. Grid boxes are coloured grey if they have less than 15 events with LST observations over the period 2000–2014. Inset histograms show the frequency of different RWR values within the global domain.

Featured publication

Gallego-Elvira, B., C. M. Taylor, P. P. Harris, D. Ghent, K. L. Veal, and S. S. Folwell (2016), Global observational diagnosis of soil moisture control on the land surface energy balance, *Geophys. Res. Lett.*, 43, DOI: 10.1002/2016GL068178.

KNOWN AND UNKNOWN UNKNOWNS

Adam Povey, NCEO Oxford

This paper outlines a best-practice assessment of uncertainty for satellite remote sensing of the environment. Uncertainty is a vital component of any data product as it highlights the data's strengths and weaknesses while providing a metric against which to compare and consolidate different estimates of the same quantity. Its importance has often been overlooked, with the terms 'error' and 'uncertainty' widely confused. Error is the difference between the value obtained and the (generally unknown) true value. Uncertainty quantifies the magnitude of error one would expect from infinitely repeating the measurement. Colloquially, uncertainty is how 'wrong' you think a measurement is and error is how 'wrong' it actually was.

Methodology

We propose five classifications of error,

- *Measurement*: The intrinsic variability in the observation (e.g. random noise);
- *Parameter*: Errors propagated from any auxiliary data used, such as a profile of temperature;
- *Approximation*: Explicit simplifications in the calculation (e.g. the use of look-up tables);
- *System*: The difference between the chosen description of the environment and reality, and;
- *Resolution*: Variations in the quantity measured at scales smaller than that observed.

Measurement and parameter errors are well represented by the traditional propagation of errors, but only describe the "unknowns" that are known and quantifiable. Approximation and system errors represent the inability of the analysis to describe the environment observed and, despite being the dominant source of error, are often impossible to quantify. Resolution errors represent the disconnect between what occurs in nature and the means by which it is observed.

The last three categories can be highly non-linear, such that traditional presentations of uncertainty do not represent the actual distribution of error. Ensemble techniques provide multiple self-consistent realisations of a data set, from which these non-linear distributions can be deduced. This is common practice in the climate modelling community, and the satellite remote sensing community should capitalise on their experience to improve communication of the uncertainty in our products. As not all errors can be quantified, it is also important to provide qualitative information, such as product user guides or quality assurance flags.

Key results and impacts

The importance of uncertainty within data is receiving wider acceptance. The European Space Agency Climate Change Initiative (which partly funded this work) requires all products to be provided with an estimate of their uncertainty. Teams such as the uncertainty working group of the AeroSAT network are investigating means of standardising and validating uncertainty across different products.

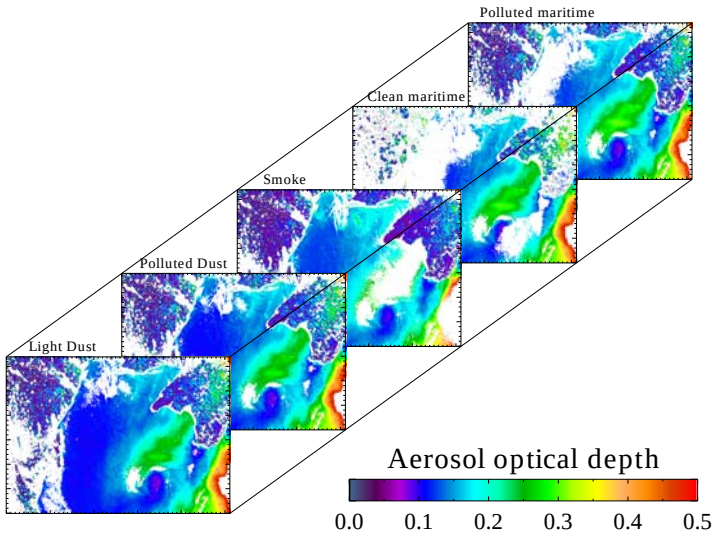

Figure 1: An ensemble of retrievals of aerosol optical depth over the Black Sea on Sep 3rd 2008. Each member assumes a different type of particle, described above each image. The plume in the centre of the field is consistent across the ensemble, indicating minimal uncertainty resulting from that assumption. There is much greater variation, and therefore uncertainty, over the hills in the top-left of the field. The members also show variable sampling due to failed retrievals (shown white), most evident in the clean maritime field, which will affect their resolution errors.

Featured publication

Featured Publication: A.C. Povey and R.G. Grainger, (2015):, Known and unknown unknowns: Uncertainty estimation in satellite remote sensing, *Atmospheric Measurement Techniques* 8, p.4669–4718, doi: 10.5194/amt-8-4699-2015.

Javier Amezcua, Peter Jan van Leeuwen, NCEO Reading; and Michael Goodliff, University of Reading

A WEAK-CONSTRAINT 4DENSEMBLEVAR: PARTS I AND II

Strong-constraint (perfect model) 4DEnsembleVar is a method at the forefront of data assimilation research and applications. This hybrid ensemble-variational method uses flow-dependent covariances in a variational framework. It also alleviates the need to compute tangent linear and adjoint models by using 4-dimensional space-time covariances obtained from an ensemble of forecasts. These covariances are usually with a static (timewise) localisation matrix. This causes problems when an assimilation window is long, and a future observation is away from the state variable it affects in the initial time.

We introduce a weak-constraint (imperfect model) 4DEnsembleVar. This allows for updates at instants other than the initial time, hence alleviating in part the problem of static localisation of 4D covariances. The method is successfully tested in three models of increasing complexity.

Methodology

We develop a weak-constraint –i.e. with imperfect model- 4DEnsembleVar. In our formulation the analysis updates occur at the initial time of the assimilation window, as well as at every observational time. We base this method in the model-bias correction formulation of weak-constraint 4DVar. This alleviates the problem of localising 4D space-time covariances with static localisation matrices.

Initial tests in the Korteweg-de-Vries system allow to illustrate the loss of information when 4D space-time sample covariances are localised in a static manner. Experiments with the 40-variable Lorenz-96 system allow us to explore the performance of our method under different parameter settings. Finally, we use a modified shallow water equation (SWE) model which allows convection to show that our method has potential in convective-scale data assimilation.

Key results and impacts

Our main contribution is the introduction of an ensemble-variational method in a weak-constraint scenario, i.e. considering the effect of model error. Our experiments suggest that having updates at times different than the start of the window helps ameliorate the problem of having badly-localised time cross-covariances.

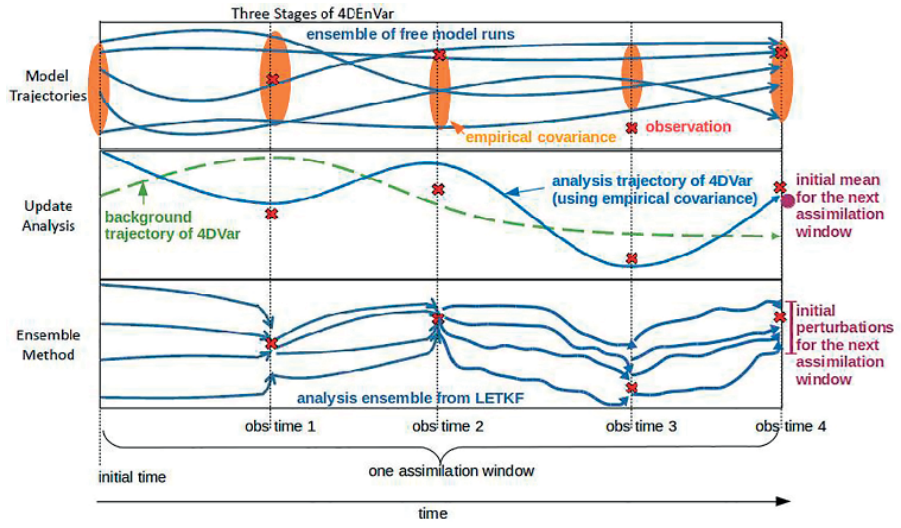

Figure 1. Schematic depicting the three stage process of 4DEnVar. First an ensemble of 'free' (DA-less) trajectories of the model is run for the length of the assimilation window. Second, the 4DVar minimisation process is performed using 4-dimensional cross-time covariances instead of tangent linear and adjoint models. Last a Local Ensemble Transform Kalamon Smoother (LETKS) is run to the end of the assimilation window to create new initial conditions for the next window. The mean of this LETKS is replaced by the solution of 4DEnVar, considered to be more accurate.

Featured publication

J. Amezcua, M. Goodliff, P. J. van Leeuwen (2016): A weak-constraint 4DEnsembleVar. Part I:

Formulation and Simple Model Experiments. Tellus A, revised version submitted in October 2016.

M. Goodliff, J. Amezcua, P. J. van Leeuwen (2017). A weak-constraint 4DEnsembleVar. Part II: A Weak-Constraint 4DEnsembleVar. Part II: Larger Models Experimentation. Tellus A, http://www.tandfonline.com/doi/full/10.1080/16000870.2016.1271565

CONSTRAINING A C-CYCLE MODEL USING MULTIPLE DATA STREAMS AND ECOLOGICAL CONSTRAINTS: A NOVEL VARIATIONAL FORMULATION

Sylvain Delahaies & Ian Roulstone, NCEO Surrey
Nancy Nichols, NCEO Reading

Carbon is a fundamental constituent of life and understanding its global cycle is a key challenge for the modelling of the Earth system. Through the processes of photosynthesis and respiration, ecosystems play a major role in the carbon cycle and thus in the dynamics of the global climate system. Over the last decade, our knowledge of the biogeochemical processes of ecosystems together with an ever-growing amount of Earth Observation systems have been extensively used to improve model predictions and uncertainty quantification.

Methodology

The data assimilation linked ecosystem model (DALEC) is a simple box model for terrestrial ecosystems simulating a large range of processes occurring at different time scales from days to millennium. In recent years many papers have demonstrated the relative merit of different inverse modelling strategies to confront DALEC with various observations types (satellite data, in situ measurements, flux towers) to estimate model parameters and initial carbon stocks to improve the prediction of carbon fluxes and characterise uncertainty. Most inverse problems are ill-posed problems: the model-observation operator which relates parameters and initial carbon stocks to the observations is rank deficient and then not all variables can be estimated, or the model-observation operator is ill-conditioned and small observational noise may lead to a solution we can have little confidence in. In both cases a regularisation mechanism is required to ensure a robust, meaningful and stable solution, the nature and efficiency of the regularisation process depending on the inverse method.

Here we adopt a variational approach (4DVAR) where a cost function measuring the mismatch between the model and observations is minimized using a gradient method based on the adjoint of the model. At Ameriflux sites we use MODIS monthly mean leaf area index (LAI) observations over a 12 years time window together with net ecosystem exchange (NEE), gross primary production (GPP) and respiration (RESP) observations from flux tower measurements. 4DVAR facilitates the diagnosis of the ill-posedness of the inverse problem: using resolution matrices, successfully adapted from the field of tomography, we can assess the resolution and stability properties of the observation operators and the regularisation terms (see figure 1).

Key results and impact

Our results confirm that the EDCs regularise an otherwise ill-posed problem and efficiently reduce the uncertainty of predicted fluxes. Our modification to DALECv2, DALEC-SP, offers an alternative to some EDCs that facilitates the variational approach. 4DVAR offers a suitable framework to solve efficiently, robustly and quickly the inverse problem for DALEC.

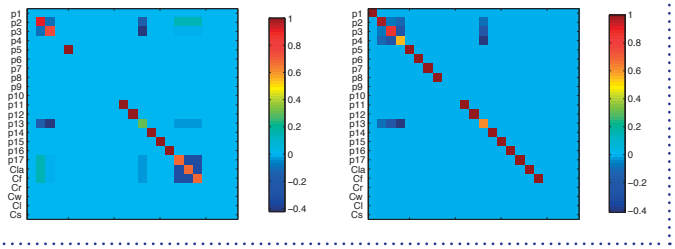

Figure 1. Resolution matrices: On the left the resolution matrix for LAI, this shows what variables can be perfectly resolved in red, variables that will have linear dependencies, and variables that will not be resolved in light blue color. On the right the resolution matrix for LAI and EDC. This shows in detail how including EDC improves resolution.

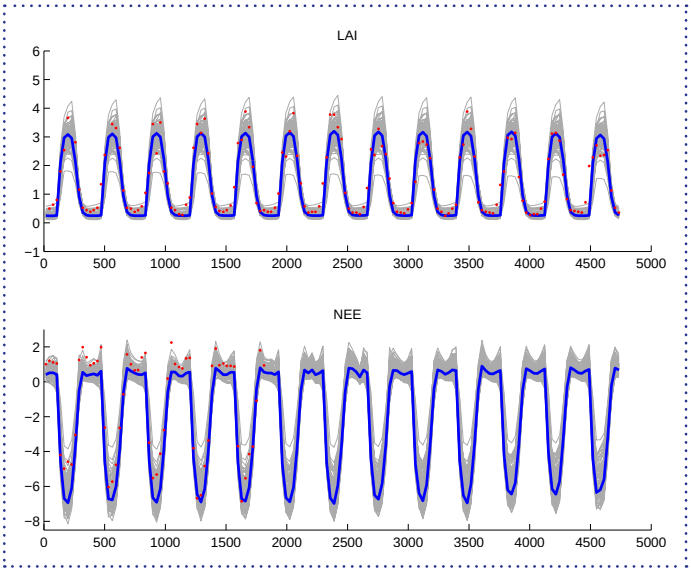

Figure 2. Model-data fusion experiment at Howland Forest (HoI, US): LAI, NEE, GPP and RESP observations are used together with EDC. The top figure shows LAI predictions, the bottom figure shows NEE predictions. The red points are the observations, the blue curves are the trajectories obtained from the optimal solution, the gray curves represent propagation of uncertainty using the posterior covariance matrix.

Featured publication

Delahais, S., I. Roulstone, N. Nichols, (2017) Constraining DALECv2 using multiple data streams and ecological constraints: analysis and application, *Geosci. Model Dev., 10, 2635–2650, 2017*

https://doi.org/10.5194/gmd-10-2635-2017

THE ASSIMILATION OF OBSERVATIONS WITH A COUPLED ATMOSPHERE-OCEAN MODEL

Alison Fowler, Amos Lawless, NCEO Reading

To improve the accuracy of sub-seasonal to decadal forecasts generated using coupled earth models, it is necessary to initialize them with a state consistent with the coupled model. To achieve this meteorological centres are investigating how to couple data assimilation (DA) schemes that have been developed for the individual components. The coupling of DA schemes introduces many new challenges. For example, coupling the atmosphere and the ocean is problematic due to the very different nature of the two different fluids in terms of density and stability and the very different coverage of observations.

Methodology

This series of work uses an idealized vertical column model of a coupled atmosphere-ocean system to give an understanding of the issues posed by different coupling strategies (Smith et al., 2015) and to focus on the issue caused by different model error growth rates in the atmosphere and ocean (Fowler and Lawless, 2016). A key problem with the latter is that this restricts the time window of observations that can be assimilated to something shorter than would be possible for ocean only DA. Due to the sparse availability of observations in the ocean this could potentially mean sacrificing the accuracy of the estimate of the ocean state in order to find a balanced coupled atmosphere-ocean state.

Key results and impact

It is found that strongly coupling the atmosphere to the ocean in the DA system introduces a faster model error growth rate in the upper ocean than would have been present in an uncoupled system. As such it is possible to get a more accurate estimate of the initial conditions, in the root mean square error sense, using an uncoupled DA system than a coupled DA system if the assimilation window is long. However, using a coupled DA system leads to a better balanced coupled atmosphere-ocean state. In particular, there is a reduced risk of initialization shock (Mullholand et al, 2015), which results in an improved forecast, despite the initial state being less accurate than that achieved by the uncoupled DA system. Therefore, coupled DA is still superior to uncoupled DA but the choice of window length should depend on whether the goal is to find the best estimate of the initial state or to produce the best forecast.

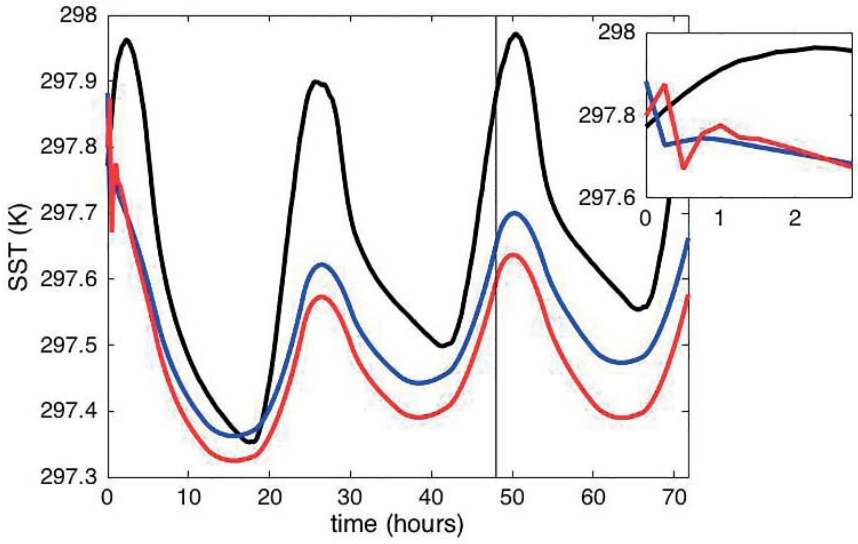

Figure 1. Three-day forecasts of sea surface temperature initialised using different DA coupling strategies; blue: coupled, red: uncoupled. These can be compared to the truth in black. The insert shows just the first three hours to highlight any initialisation shock. Can see that the uncoupled DA scheme gives most accurate estimate of SST at the initial time but has unrealistic fluctuations as it returns to the model trajectory and at later times gives a poorer forecast than the coupled DA scheme.

Featured publication

A. M. Fowler, A. S. Lawless (2016); An Idealized Study of Coupled Atmosphere–Ocean 4D-Var in the Presence of Model Error. *Mon. Wea. Rev.*, 144, 4007–4030, doi: 10.1175/MWR-D-15-0420.1.

Additional science references

P.J. Smith, A. M. Fowler, A. S. Lawless (2015); Exploring strategies for coupled 4D-Var data assimilation using an idealised atmosphere-ocean model. Tellus A, doi:http://dx.doi.org/10.3402/tellusa.v67.27025.

Mullholland, D. P., P. Laloyaux, K. Haines, and M. Balmaseda, 2015: Origin and impact of initialization shocks in coupled atmosphere–ocean forecasts. Mon. Wea. Rev., 143, 4631–4644

Peter Jan van Leeuwen, Phil Browne, NCEO Reading; Matthew S. Lang, University of Reading

SYSTEMATIC MODEL IMPROVEMENT USING DATA ASSIMILATION

In many geoscience models parameterisations are used to simulate missing physics, chemistry, and/or biology. These can be due to a lack of scientific understanding or a lack of computing power available to incorporate all details of the processes. Standard data assimilation methods for parameter estimation fail when estimating parameterisations. However, we found such a method, opening the way for systematic model improvement through data assimilation.

Methodology

We need to use a data-assimilation method that can handle errors in the model equations. First observations are assimilated into the model over a period of time. The data assimilation corrects the evolution of each model variable at each time step at each model grid point, and these corrections are stored. In practice these corrections are calculated as the difference between a pure model forecast for one time step, starting from the data-assimilation analysis at a time point, and the result of the data assimilation after that time step, as depicted in figure 1.

The resulting correction fields contain a part that is a function of the model variables, which will be the new parameterization, and a random part that is not related to the model variables. We find that function by asking experts in the field to come up with a range of possible parameterisations, and we use the Bayesian Information Criterion (BIC) to find the best parameterisation, or the best combination, including error estimates.

We tested this method on a very simple one-dimensional nonlinear advection equation for velocity. We assume that the model is linear, while we generated pseudo observations from the full nonlinear model. The data-assimilation will correct the linear model evolution, resulting in a correction field as depicted in figure 2. From this we extract the best parameterisation using the BIC. The method successfully changes the linear model to the correct nonlinear model.

Key results and impacts

We have developed a new method for systematic model improvement based on data assimilation. An advantage of our method is that we estimate parameterisations at the level of the model equations, instead of comparing model-generated fields with observational fields. In the latter case it is extremely hard to find the cause of the difference. Furthermore, our method provides error estimates on the best parameterisations. We have secured funding to test the method on the operational weather prediction model of the Met Office.

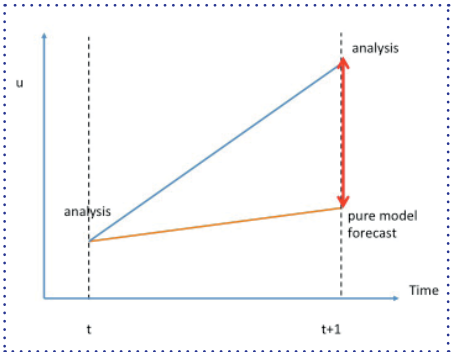

Figure 1. Illustration of the main idea. Starting from the data-assimilation analysis at time t do one pure model forecast for one time step (yellow line) and compare this with the time evolution of the data-assimilation analysis over that time step (blue line). The difference (red arrow) contains information on the missing parameterization. This calculation is repeated for each model variable at each time step and at each grid point to generate the full correction field for the model.

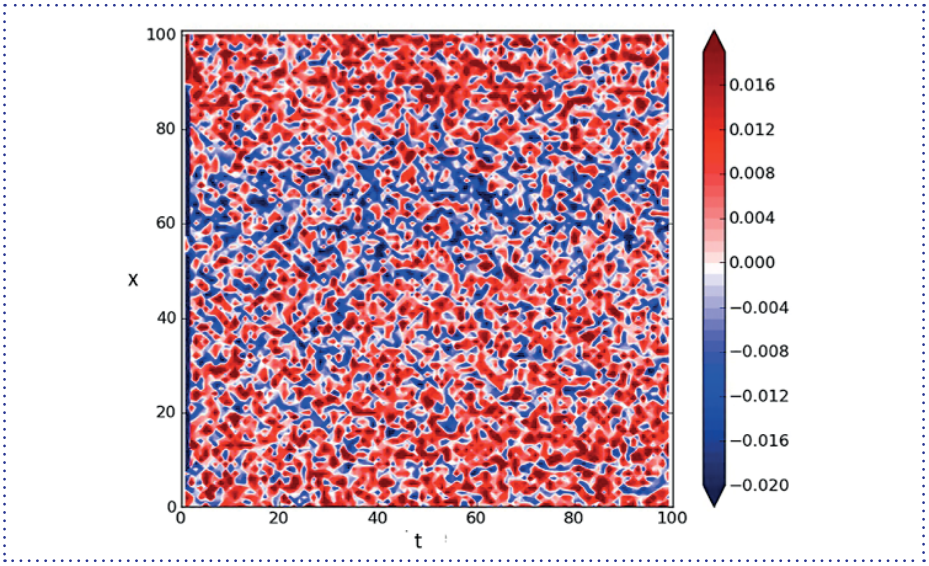

Figure 2. Example of a correction field for the one-dimensional advection of velocity. The horizontal axis is time, the vertical axis denotes space, and we started the run with a pure sine wave with a wavelength equal to the model domain (100 grid points). The noise comes from observation errors and initial errors in the model equations. This noisy field contains the difference between the velocity using linear model and the velocity using the correct nonlinear model, for each time and space point. It shows that the wave moves too slow in the blue area, and too fast in the red area. This difference is a function of the velocity, in this case a combination of linear and nonlinear velocity advection. The BIC is able to find these correct advection terms out of a whole family of possible functions of the velocity (e.g. linear terms, diffusion terms etc.).

Featured publication

Lang, M.S., P.J. van Leeuwen, and P. Browne, 2016: *Tellus* A, 68, 29012, http://dx.doi.org/10.3402/tellusa.v68.29012.

Joanne Waller, Sarah Dance, Nancy Nichols NCEO Reading;
D. Simonin, G. A. Kelly, S. P. Ballard, Met Office

DIAGNOSING OBSERVATION ERROR STATISTICS FOR SEVIRI OBSERVATIONS

With the development of convection permitting numerical weather prediction the efficient use of high resolution observations in data assimilation is becoming increasingly important. Observations, such as radiances from the Spinning Enhanced Visible and Infrared Imager (SEVIRI) onboard the Meteosat Second Generation satellite, are now routinely assimilated in operational systems. However, to avoid violating the assumption of uncorrelated observation errors it is necessary to reduce the density of the observations. In this work we characterise both inter-channel and spatial error correlations for SEVIRI observations. It is expected that improvements in the description of observation errors will allow the quantity of observations used to be increased and could lead to a significant enhancement of forecast quality.

Methodology

In this work we use the diagnostic of Desroziers et al. (2005) to calculate both spatial and inter-channel observation error statistics for SEVIRI radiances that are assimilated into the Met Office 1.5km model. Further to considering the error statistics across the full model domain, we also demonstrate the variation of results across the geographical domain and highlight the enhanced understanding that this can bring. We note that the diagnostic used in this study is sensitive to the forecast and observation error statistics used in the assimilation, although, with careful interpretation of the results, it can still provide useful information (Waller et al. 2016).

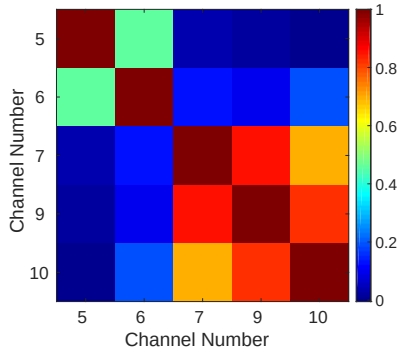

Figure 1. Estimated observation error correlation matrix for SEVIRI channels assimilated into the Met Office high resolution 1.5km model. Channels 5 and 6 are upper level water vapour channels, channels 7, 9 and 10 are surface channels.

Key results and impacts

The results suggest that the operational variances are much too large, with the estimated variances being as low as one tenth of those currently used. We find that the horizontal observation error correlations range between 30km and 80km dependent on the observation channel; this is larger than the operational thinning distance of 24km. The upper level water channels have significantly correlated inter-channel errors, as do the surface channels. We find, for the surface channels, that the observation error variances and inter-channel correlations are larger in coastal areas of the domain; this is the result of assimilating mixed pixel (land-sea) observations. As a result of this work the Met Office has improved the SEVIRI observation quality control and observation processing procedures.

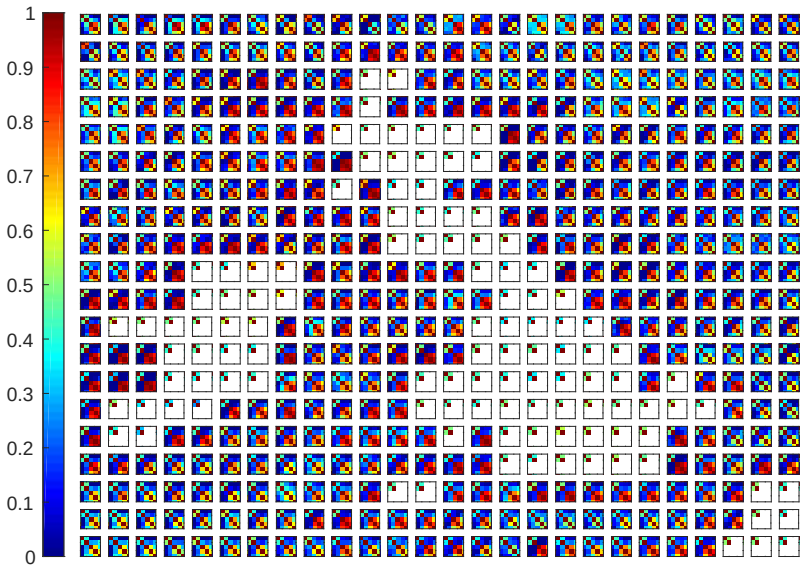

Figure 2. Estimated observation error correlation matrices for assimilated SEVIRI channels (as in Figure 1) for sub domains of the Met Office high resolution model.

Featured publication

Waller, J.A.; Ballard, S.P.; Dance, S.L.; Kelly, G.; Nichols, N.K.; Simonin, D. Diagnosing Horizontal and Inter-Channel Observation Error Correlations for SEVIRI Observations Using Observation-Minus-Background and Observation-Minus-Analysis Statistics. *Remote Sens.* 2016, 8, 58 doi: 10.3390/rs8070581.

Additional science references

Desroziers G., Berre L., Chapnik B. and Poli P. Diagnosis of observation, background and analysis error statistics in observation space *QJRMS*., 131:3385–3396, 2005.

Waller J.A., Dance S.L., Nichols N.K. Theoretical insight into diagnosing observation error correlations using observation-minus-background and observation-minus-analysis statistics. *QJRMS*. 2015a doi:10.1002/qj.2661.

Victoria Bennett and team,
NCEO Centre for Environmental Data Analysis, STFC

SUPPORTING THE EO SCIENCE COMMUNITY WITH DATA AND PROCESSING FACILITIES

The Centre of Environmental Data Analysis (CEDA) has continued to support the NCEO and wider EO research community with access to key datasets and a processing and analysis environment on the JASMIN infrastructure.

In 2016, CEDA curated nearly 3PB of data and supported over 30,000 users:

Acquiring and disseminating Sentinel data

Sentinel satellites 1A, 1B, 2A, 2B and 3A of the Copernicus Satellite programme are already in space, with further satellites to follow in the coming years. The Sentinels are collecting unprecedented volumes of data (approximately 8 Terabytes/ day), opening opportunities for new and improved scientific and commercial applications. As part of the UK's collaborative ground segment, CEDA is responsible for a mirror archive of global Sentinel data to serve the UK academic community. To date, over 1 Petabyte (920 Terabytes) have been acquired and included in the CEDA archive for users to access, with Sentinel 3 data expected in late 2016. The UK Earth Observation Science community is increasingly making use of these data, and CEDA is developing data search and access services to make it easier for scientist to interact with the data.

Supporting research projects using JASMIN

The JASMIN super-data-cluster has been extensively used by NCEO scientists for analysing and processing datasets for international science. Recent high profile projects include:

Thematic Exploitation Platforms for ESA

Deployed in the JASMIN cloud TEPs offer a one-stop shop for remote sensing services for academic and commercial sectors such as forestry and polar. They offer access to pre-processed satellite and ancillary data, computing power, software access and hosting.

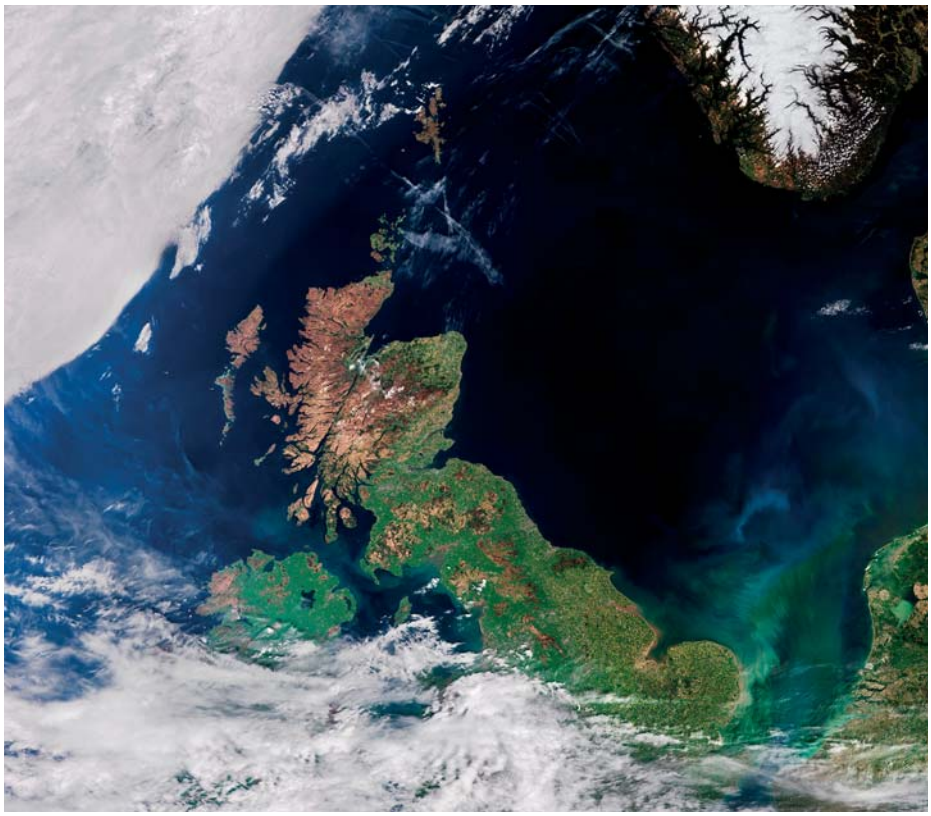

Figure 1. Sentinel-3 Image of UK, contains modified Copernicus Sentinel data [2016/ processed by ESA].

Developing the Climate Change Initiative central archive and open data portal

CEDA and partners in Telespazio Vega, CGI and University of Reading, have developed and launched the "CCI Open Data Portal" for the European Space Agency's Climate Change Initiative Programme. Datasets of long-term global climate relevant parameters, essential climate variables, derived from satellite data by CCI science teams around Europe, have been gathered into a central data archive and made available through a range of download mechanisms (see cci.esa.int). The data are also available through the CEDA archive and for direct access by users of the JASMIN infrastructure, alongside CEDA's other data holdings.

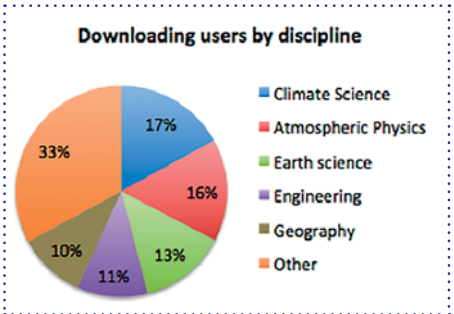

Figure 2. Downloading users by discipline

The Climate Change Initiative exploits Europe's Earth Observation assets to generate robust long-term global records of essential climate variables such as greenhouse-gas concentrations, sea-ice extent and thickness, and sea-surface temperature and salinity.

Victoria Bennett and team,
NCEO Centre for Environmental Data Analysis, STFC

SUPPORTING THE EO SCIENCE COMMUNITY WITH DATA AND PROCESSING FACILITIES

Figure 3. The CCI Open Data Portal

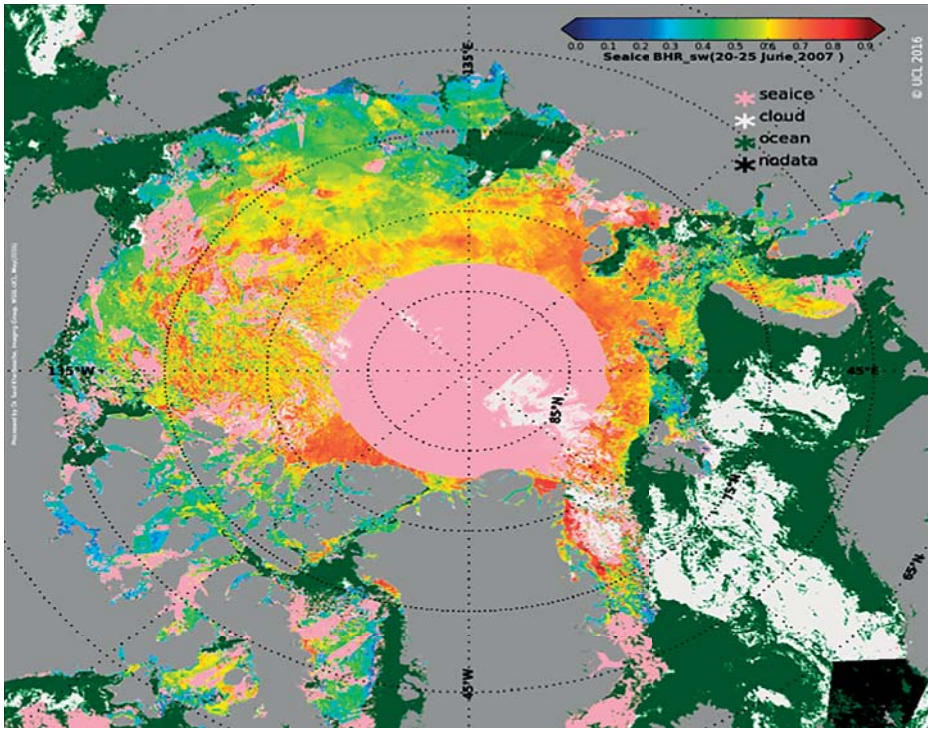

Figure 4. QA4ECV (Prof Jan-Peter Muller UCL)

Quality Assured Earth Observation Data: the QA4ECV project

Satellites are providing a continuous global measurement of the land surface and atmospheric chemistry; revolutionising the way scientists assess climate change and air quality. New essential climate variables are being generated on JASMIN as part of the QA4ECV project. This involves processing hundreds of terabytes (TB) of data to generate a 35 year record of quality assured global land surface products from European and US EO instruments.

The time taken to process these satellite datasets has been dramatically improved (by 2 orders of magnitude); one example showed completion in just 3 days – 81 times faster than on a local machine. Many other processing tasks show similar benefits, e.g. circa 100 times faster processing. A dedicated project workspace (>700 TB) on JASMIN has been funded through the UK NERC Big Data programme. The project has also benefited from a dedicated high-performance transfer server, which has allowed input datasets (MODIS, MISR) to be transferred from US data providers onto JASMIN very efficiently, at rates up to 28 TB/day.

Combining model simulations with observations of air pollution

Understanding the balance between natural and anthropogenic chemistry is vital when observing air quality, especially over countries known for their poor air quality, such as India. Formaldehyde is a product of volatile organic compounds that are a precursor for tropospheric ozone and organic aerosol, both of which are harmful at elevated concentrations to human health. JASMIN is being used to run the GEOS-Chem model at 25km over India to interpret satellite observations for formaldehyde from the Ozone Monitoring Instrument (OMI).

The technical challenge is to run the model at the necessary spatial resolution to pick up individual cities over India; the advantage of using JASMIN is that the data and meteorology are collocated so there is a seamless transition between model analysis and data analysis that is required to achieve these cutting-edge science objectives.

Reprocessing satellite missions on JASMIN; measuring greenhouse gases from space

Carbon dioxide (CO_2) and methane (CH_4) are the two most important anthropogenic greenhouse gases (GHGs). The capability to accurately and frequently measure them on a global scale is vital to understanding their impact upon the climate system. The requirement for large spatial coverage and regular sampling means that satellite observations are a key component of such a monitoring system. These observations, combined with atmospheric transport modelling, help to improve our knowledge of the sources and sinks of gases, ultimately improving future climate predictions.

A complex algorithm is required to infer the amount of GHGs in a satellite remote sensing measurement. For new satellites such as the NASA Orbiting Carbon Observatory-2, this number can be in excess of 30 million measurements each month (24 measurements every second) – necessitating vast processing capabilities and 10-100s TBs in storage.

JASMIN enabled the ESA GHG-CCI project to reprocess the entire GOSAT mission (2009 – present) with the improved CO_2 algorithm within several weeks, as opposed to the many months that it would take locally. The intensive

Victoria Bennett and team,
NCEO Centre for Environmental Data Analysis, STFC

SUPPORTING THE EO SCIENCE COMMUNITY WITH DATA AND PROCESSING FACILITIES

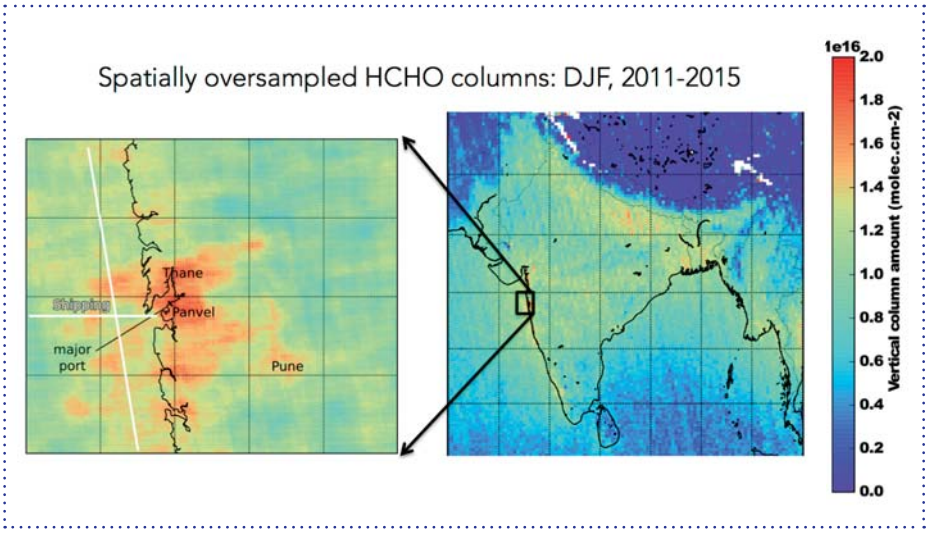

Figure 5. Formaldehyde columns (Dr Luke Surl and Prof Paul Palmer, NCEO Edinburgh)

number of measurements and data volume provide a huge challenge for individual institutions. Future missions, such as Sentinel 5P, are expected to see the number of measurements and data volume preclude any local retrieval; thus a national capability is vital in continuing to produce important climate datasets.

Emissions from Smoke Pollution

Agricultural or landscape burning is carried out to clear the land for future uses; however the associated emissions of smoke pollution can be extremely harmful. For example, widespread burning of crop residues is suspected of contributing significantly to China's air quality problems, including in the mega-cities of Shanghai and Beijing. Such emissions can be observed from space.

New data from the US instrument VIIRS and Himawari-8 Japanese satellites are being used to estimate fire activity, exploiting their high spatial resolutions (existing datasets are known to under-represent the number and extent of fires in agricultural regions). These new data are tens of TBs in volume. JASMIN is essential to processing these large datasets, using new algorithms, successfully built, tested and optimised to process the data. Initial work shows that existing inventories may be underestimated by around an order of magnitude.

This work is helping to support the UK's official development assistance (ODA) which aims to assist science and innovation partnerships for economic development in overseas countries. The next steps will involve a final smoke emission inventory, which will be used as a key input to improve future air quality models; these could then be used by policy makers to appropriately target how air quality could be improved with legislation.

Deriving the impact of fire on vegetation from EO data

Fire is ubiquitous in the Earth System. There is a pressing need to assess fire and its role in the carbon cycle as well as its impact on economics and biodiversity. UCL scientists have developed methods to quantify the impact of fire on vegetation. These metrics are important as they allow us to see whether over the satellite record, fire impact has changed. In order to produce a decadal dataset of fire impacts, large amount of input data needs to be processed.

This work is normally constrained by both storage space and processing capabilities. JASMIN is a fantastic tool on both counts; not only is there adequate storage, but accessing large datasets is also very efficient – allowing complicated processing on typical tasks to be done in a few weeks, instead of months to years. Without JASMIN this intensive processing would involve large amounts of time and effort, but now scientists can focus their time on addressing the science rather than processing logistics. These datasets will be used to improve greenhouse gas emission estimates from wildfires, in the past and in the future.

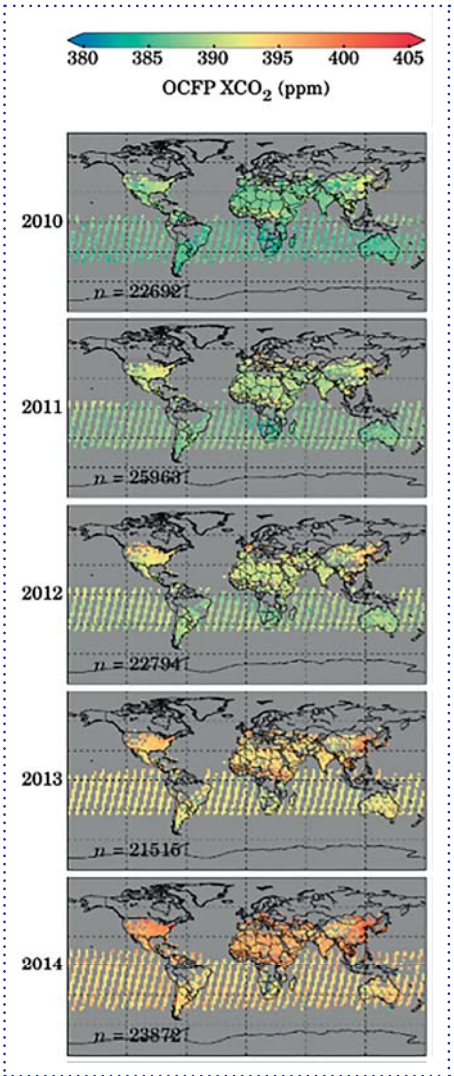

Figure 6. Greenhouse gases from Space (Dr Robert Parker, Dr Peter Somkuti, Dr Hartmut Boesch, NCEO Leicester)

Victoria Bennett and team, NCEO Centre for Environmental Data Analysis, STFC

SUPPORTING THE EO SCIENCE COMMUNITY WITH DATA AND PROCESSING FACILITIES

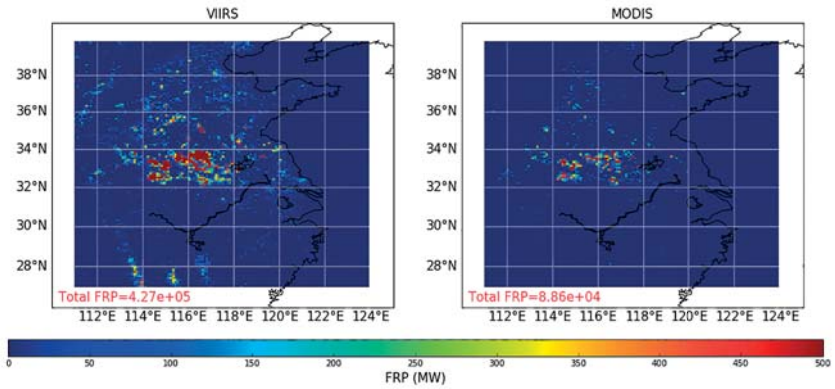

Figure 7. Remote Sensing from Space of Smoke Emissions (Tianran Zhang, Weidong Xu, Jiangping He and Prof Martin Wooster, NCEO King's College London)

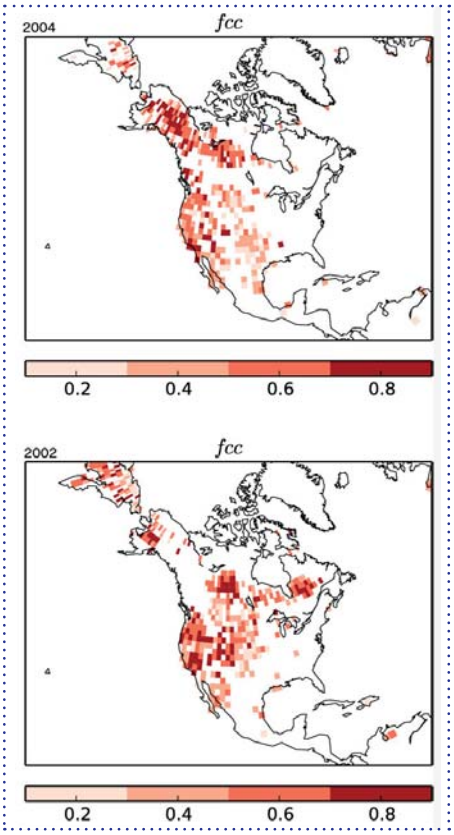

Figure 8. Estimating wildfire gas emissions from Earth observation (Dr Jose Gomez-Dans, Prof Phil Lewis and James Brennan, NCEO UCL)

Sea Surface Temperature from Space

Sea surface temperature (SST) provides fundamental information on the global climate system; it is an essential parameter in weather and climate prediction. Earth observation (EO) data collected via satellites provides global observations of SST, this can then be used in the running, validation, and interpretation of high resolution atmospheric and ocean models.

The ESA Climate Change Initiative (CCI) programme utilises circa 180TB of raw EO data currently archived at CEDA, producing circa 50TB of high level products. JASMIN allows scientists to generate 30+ years of datasets in just a few days, rather than months or years (with interim products, the SST-CCI alone needs 260TB of group workspace for product development).

The SST section of the Copernicus Climate Change Service (C3S ST) will also make use of JASMIN to obtain near-real time satellite data and generate short delay products useable by ECMWF and others – ensuring no duplication of effort.

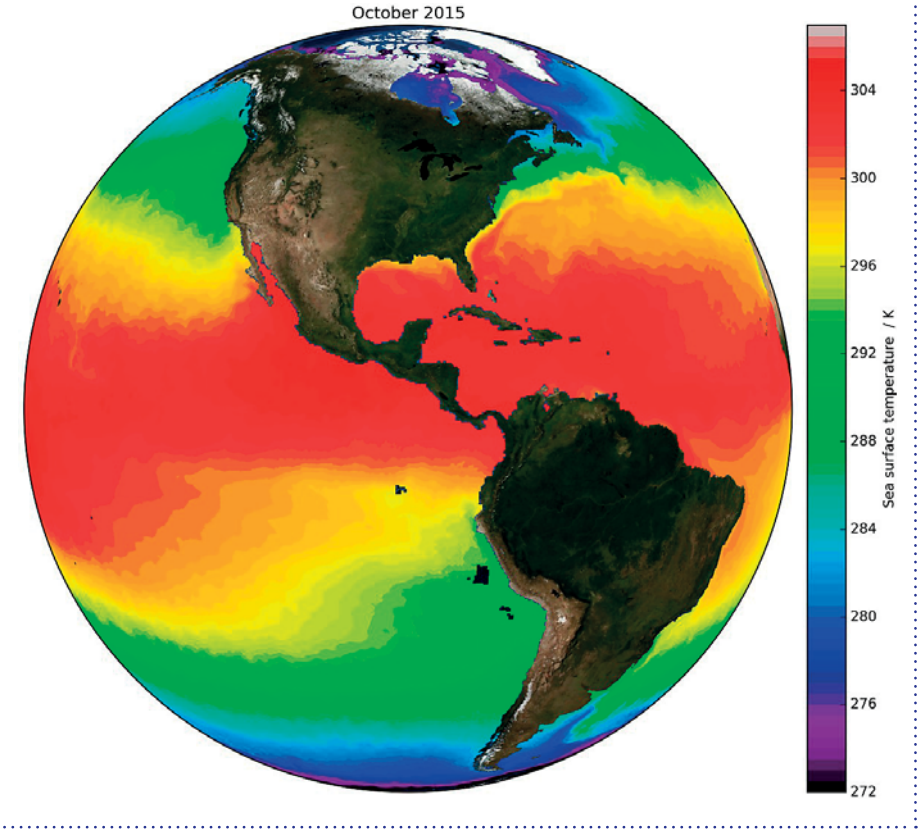

Figure 9. Using Global Sea Surface Temperature Measurements (Prof Chris Merchant, Dr Owen Embury, NCEO Reading)

NERC Earth Observation Data Acquisition and Analysis Service (NEODAAS)

THE NERC EARTH OBSERVATION DATA ACQUISITION AND ANALYSIS SERVICE (NEODAAS)

Serret et al. (2015) in *Nature Communications* is one of 65 peer-reviewed publications and 17 NERC grant, PhD and centre/survey projects in 2015 which were supported by data from NEODAAS. They used data from the Atlantic Meridional Transect (AMT) series of cruises to investigate the metabolic state of the ocean gyres, specifically whether ocean gyres are dominated by photosynthesis or respiration. They showed that the state may be different for different gyres, in that the respiration rate may vary independently of the photosynthesis rate.

NEODAAS supports the annual AMT cruises with near-real time and synoptic data and for Serret et al (2015) provided consistent composite images with cruise tracks for AMT 11 –22. AMT is used as a sampling platform for NCEO ocean scientists and AMT26 between September – November 2016 will be carrying Dr Giorgio Dall'Olmo and Dr Bob Brewin who will be sampling bio-optical characteristics between the UK and the south Atlantic. AMT26 has special significance since in collaboration with ESA data will be obtained for validation of the ESA Sentinel 2A MSI and Sentinel 3A OLCI and SLSTR sensors.

Tracks of Atlantic Meridional Transect (AMT) cruises 11–18 and 21–22 overlaid on SeaWiFS chlorophyll *a* composites. After AMT11 (September–October 2000), cruises took place biannually from May 2003 (AMT12) until October 2005 (AMT17); AMT18, 21 and 22 took place in September–October 2008, 2011 and 2012, respectively. Earth observation data produced by the ESA Ocean Colour Climate change Initiative, courtesy of the NERC Earth Observation Data Acquisition and Analysis Service, Plymouth, the Ocean Biology Processing Group, NASA and European Space Agency.

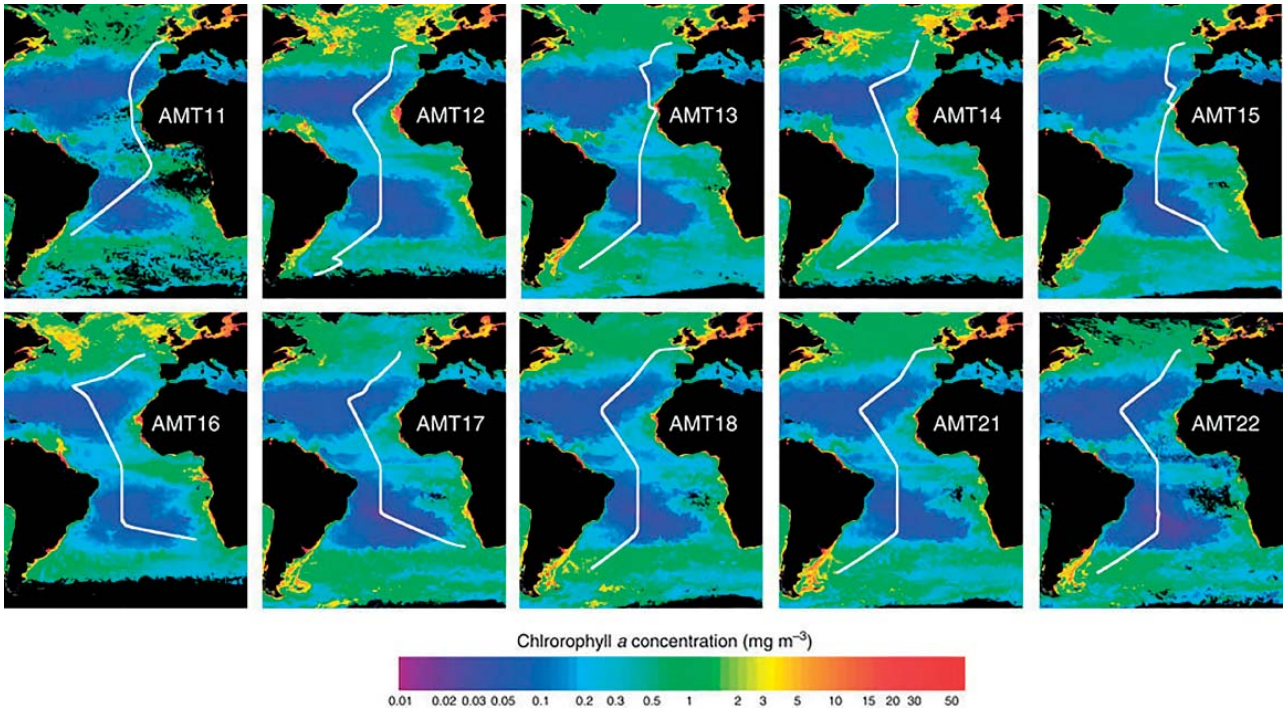

Figure 1. The AMT cruises.

Featured publication

Pablo Serret, Carol Robinson, María Aranguren-Gassis, Enma Elena García-Martín, Niki Gist, Vassilis Kitidis, José Lozano, John Stephens, Carolyn Harris & Rob Thomas; *Nature Communications* 6, Article number: 6961 (2015) doi: 10.1038/ncomms7961 http://www.nature.com/articles/ncomms7961.

http://www.nature.com/articles/ncomms7961/figures/1.

This publication was produced using data provided by NEODAAS.

Alasdair MacArthur,
NCEO FSF Edinburgh

THE FIELD SPECTROSCOPY FACILITY

FSF supported Dr Coomes and Nunes, University of Cambridge in a NERC Doctoral Training project investigating the variation in plant functional traits. Recent analyses of traits based on thousands of tree species reveal strong variation at the global scale, but these studies tend to focus on interspecific variation. Spectranomic is a developing technology for estimating the traits of fresh leaves by field spectroscopy (FS). Few studies have evaluated its potential for assessing inter- and intra-specific trait variability community ecology. Results indicate that most leaf traits varied greatly among species. The effects of soil type were generally weak by comparison: macronutrient concentrations were greater on alluvial soil, micronutrient concentrations (Ca, Mg, B, Mn and Zn) were greater on chalk soil, while structural properties were invariant of soil type. FS provided accurate estimates of many species-level trait values. Leaf mass area, foliar water content, total phenolics, Si, K, B and N concentrations, efficiency of photosystem II, and the pigments chlorophyll a, chlorophyll b and carotenoids were accurately predicted using this method. Interspecific and within-species variation were detected well for most foliar traits, however FS was less effective at picking up subtle variation of rock-derived nutrients between soil types.

In an international collaboration with DLR (Germany) and University of Poznan (Poland) FSF's Alasdair MacArthur established a Sentinel-2 cal/val site at Rzecin, Poland for long term Earth observation (EO) and atmospheric correction research. This location is particularly suited for northern European optical EO as it has an average 40 days with cloud cover less than 20% and only about 120 days with cloud cover higher than 80%. The FSF CIMEL is now installed and the site included in the DLR Sentinel-2 validation and NASA AERONET networks http://aeronet.gsfc.nasa.gov/new_web/photo_db/POLWET_Rzecin.html.

At this site the utility and reliability of the dual-field-of-view (DFOV) spectrometer system for Earth sun induced fluorescence and radiant flux measurements, developed by MacArthur and colleagues, will be tested. The system will be used concurrently to validate Sentinel-2 Earth surface reflectance products. Further hardware developments are in progress to develop a sunphotometer configuration of the DFOV spectrometer system. Hyperspectral atmospheric measurements will be made to derive aerosol optical thickness and water vapour content for the validation of the atmospheric correction of Sentinel-2, Sentinel-3 images and O_2 absorption for FLEX images.

Figure 1. Mateus Nunnes and colleague making leaf spectral measurements at an Indonesian forest site.

Figure 2. FSF CIMEL mounted on tower at wetland research site Rzeci, Poland.

Sophie Hebden, NCEO Leicester

THE JOINT UK GEO/CEOS OFFICE

NCEO is working on behalf of the UK Earth Observation community to interface to two major international initiatives: the Group on Earth Observations (GEO) and the Committee on Earth Observation Satellites (CEOS).

GEO is a voluntary partnership of 102 governments and the European Commission, plus 103 organisations, working to make EO data and resources freely available to help with better policy-making. It is leading a worldwide effort to create a data portal called the 'Global Earth Observation System of Systems' (GEOSS) to link EO resources worldwide across multiple Societal Benefit Areas. Defra is the UK policy lead for GEO.

CEOS (Committee on Earth Observation Satellites) is GEO's sister coordination body, which aims to coordinate civil space-based EO programmes. The UK Space Agency has responsibility for leading on CEOS.

What have we done this year?

This year NCEO set up a joint UK GEO/CEOS Office to coordinate UK activities relating to these two initiatives alongside Defra and the UK Space Agency. The Office is working to increase the visibility of GEO to the UK EO community, facilitating and coordinating the UK's inputs to GEOSS. We disseminate information about CEOS and GEO activities and solicit community feedback, as well as host GEO and CEOS events in the UK.

This year we organised the GFOI (Global Forestry Observation Initiative) Policy Forum in London (6 September 2016), and the Space Data Coordination Group for GFOI – SDCG-10 in Reading (7–10 September 2016). The meetings were very successful but tinged with great sadness due to the death of Professor Jim Penman who chaired the Advisory Group for GFOI and led GFOI's work on developing a set of methods and guidelines to assist REDD+ countries in developing their national forest monitoring systems.

Jim chaired the GFOI Methods & Guidance Documentation Advisory Group (AG) pictured here: Jim is second from the left on the front row.

The Office has also supported work to share metadata for UK EO datasets stored on data.gov.uk to the GEOSS data portal. From the September onwards, 23,458 UK metadata records are being harvested to the GEOSS data portal, including numerous NCEO datasets available on CEDA. These records are shared as Open Data by default and are available as part of the GEOSS Data Collection of Open Resources for Everyone (Data-CORE).

We announced our contributions to data-sharing and GFOI at the GEO plenary meeting held in St Petersburg 9–10 November 2016. The UK has a voice at the heart of GEO decision making with delegates on the GEO Executive Committee (as part of the European caucus) including Dr Iain Williams, Defra Deputy Chief Scientific Adviser, and the GEO Programme Board. The UK is also an active participant on the European Commission's High Level Working Group.

Web Links:

The GEOSS Data Portal: http://www.geoportal.org/.

The Joint UK GEO/CEOS Office: https://www.nceo.ac.uk/innovation/nceo-geo/.

Global Forestry Observation. Initiative (GFOI) http://www.gfoi.org/.

NCEO ANNUAL SCIENCE CONFERENCE 2016

Jan Fillingham, NCEO Training, Communications and Events Manager

NCEO colleagues were involved in many conferences during 2016, including EGU, the Showcase for DEFRA's EO Centre of Excellence, ESA Living Planet Symposium, RSPSoc, and the Challenger Society for Ocean Conference. NCEO held training workshops, including the Researchers Forum in Leicester, and NCEO colleagues hosted the 5th International Symposium on Data Assimilation (ISDA) in Reading. With the UKSA we hosted the Global Forest Observation Initiative meetings in London and Reading.

NCEO also took part in the NERC *Into the Blue* public engagement events, including the visit by RRS Discovery to Liverpool, the keel laying ceremony for the new Polar Ship RRS Sir David Attenborough, and the *Into the Blue Manchester* event at the Airport Runway Visitor Centre.

There were many more outreach activities around NCEO's EO Detective project – linked to Tim Peake's *Principia* trip to the International Space Station. Read more about this and the results of the EO Detective competition on page 41.

One highlight of the year was the NCEO Annual Science Conference. 130 people attended NCEO's 2016 Science Conference in Warwick, 29 June – 01 July. Plenary sessions included: Energy and water cycles; Towards Sentinel Data; Atmospheric pollution and the land emissions; Environmental forecasting and data assimilation; International science; Climate data for the Earth system; Instruments and Facilities Science; and the Carbon Cycle. We were joined by people from the UK Space community for an afternoon's discussion on Copernicus Science and Future Missions; planned before the country voted for Brexit, it became an important forum for reaffirming our commitment to collaboration.

Talks and poster presentations were selected from submitted abstracts, and the evening poster sessions proved to be very popular. And whilst most of the conference was plenary, we managed to squeeze in a one-and-a-quarter hour breakout session for discussions on DA strategy; Global challenges; NERC Services, Facilities and Data Centres; Outreach; Visualising EO Data; and Impact.

Poster prizes were awarded to the CEDA group and to Peter Somkuti. Prizes for best talks by early career scientists were awarded to Jake Gristey and Matthew Hethcoat. Summaries of these talks follow.

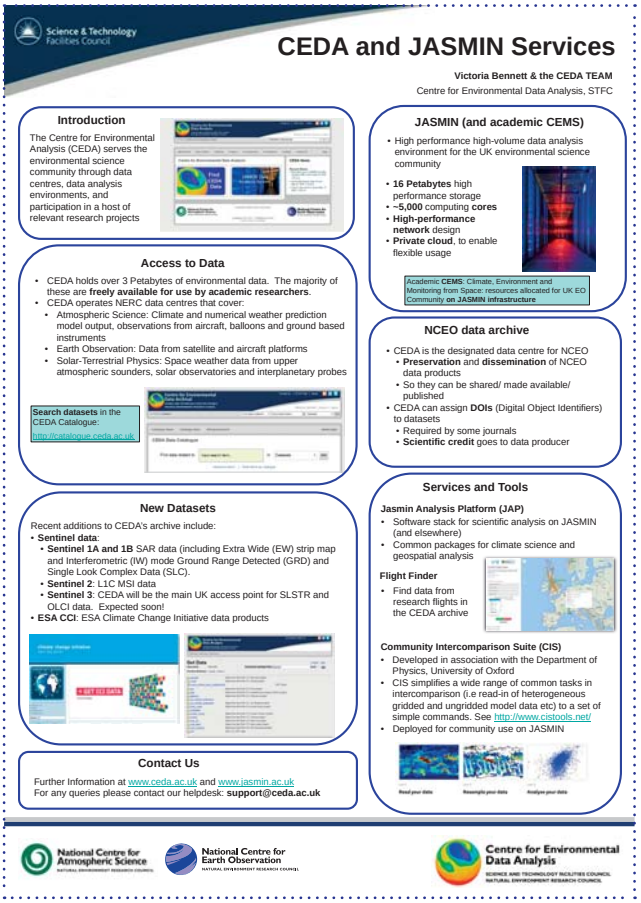

Joint winning poster – by the CEDA team

Joint winning presentation – by Jake Gristey

OBSERVING THE EARTH'S RADIATION BUDGET FROM A CONSTELLATION OF SATELLITES

Jake Gristey, NCEO Reading

The total outgoing radiation at the top of the atmosphere (TOA) provides an important fingerprint of climate change. If our climate system is in equilibrium, the total outgoing radiation at TOA is the same as the incoming radiation. If the total outgoing radiation is less than the incoming energy at TOA, the Earth is imbalanced and its temperature will warm. Since this imbalance is the primary driving force for climate change, the ability to accurately measure TOA radiation is crucial for understanding the underlying radiative processes and for better modelling the climate system. However, it remains challenging to monitor the TOA radiation at low costs with sufficient spatial coverage and temporal resolution.

To address this issue, we explore a viable and sustainable observation strategy – a constellation of satellites, by capitalising on technology revolutions in small satellites and sensor miniaturisation.

Methodology

Using a series of simulation experiments, we evaluated the potential of a constellation that consists of 36-satellites each hosting a wide field-of-view broadband radiometer with a 6000 km footprint (Figure 1a). As shown in Figures 1(b)-(d), this constellation provides sufficiently dense global coverage after just one hour, allowing us to recover a global map of outgoing radiation. Unlike the featureless raw observations, the hourly recovery at an enhanced spatial resolution of 1000 km is able to capture synoptic-scale features such as tropical cyclones in the central Pacific and mid-latitude frontal systems. Based on one day of simulations, the uncertainty in the hourly recovered radiation is 0.16 ± 0.45 W m^{-2} for reflected shortwave irradiance and 0.13 ± 0.15 W m^{-2} for emitted longwave irradiance.

Further, we further conducted a number of sensitivity tests to fully understand the impacts of potential issues like calibration, reduced number of satellites due to limited resources, and the anisotropic nature of radiation. Not surprisingly, the success of the recovery will rely on calibration that ensures low systematic instrument biases, and on a sufficient number of satellites that ensures dense hourly sampling of the globe.

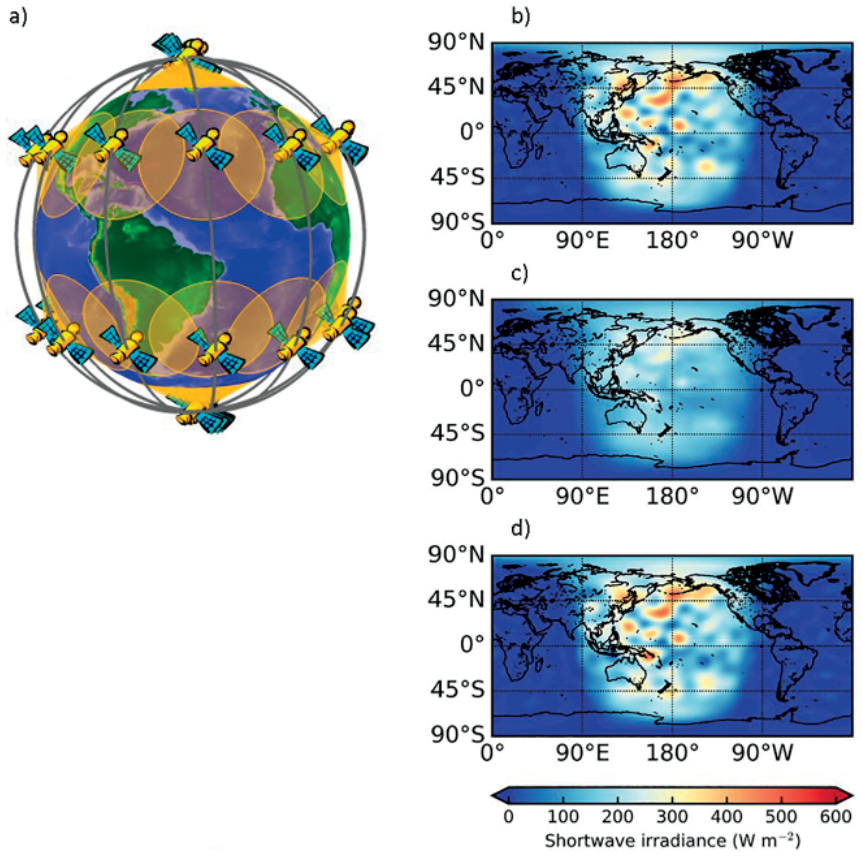

Key results and impacts

Along with good calibration and sufficient satellites, this study demonstrates that the concept of a constellation provides an unprecedented sampling capability and has a clear potential for improving observations of Earth's outgoing radiation.

Figure 1: A series of simulation experiments have been conducted using TOA outgoing irradiance fields from the Met Office global numerical weather prediction model, with a constellation of 36 satellites, a snapshot shown in (a). (b) The modelled outgoing shortwave irradiance at TOA is served as the "truth" in the experiments. (c) Synthetic satellite measurements of outgoing shortwave radiation, treated as raw observations. (d) Recovered TOA outgoing shortwave irradiance at a 1000km spatial resolution.

Featured publication

Gristey, J. J., J. C. Chiu, R. J. Gurney, S.-C. Han, and C. J. Morcrette (2017), Determination of global Earth outgoing radiation at high temporal resolution using a theoretical constellation. of satellites, J. Geophys. Res. Atmos., 122, doi:10.1002/2016JD025514.

DETECTING TROPICAL SELECTIVE LOGGING WITH OPTICAL AND RADAR SATELLITE DATA

Matthew Hethcoat, NCEO Sheffield

Earth's forests are being rapidly lost and degraded from a host of anthropogenic factors.

While satellite monitoring of deforestation has achieved accuracies >90% in recent years, techniques to detect and quantify the extent of selective logging have remained elusive. This project seeks to map and quantify the amount of selectively logged tropical forest in the Amazon basin, relying on a detailed spatial dataset of logging locations from a study site in Rondônia, Brazil.

Methodology

Our initial findings suggest an encouraging ability to identify regions that have been selectively logged at low intensities (1–2 trees ha^{-1}). However, an unacceptably high false alarm rate (i.e., unlogged areas being classified as logged) has thus far limited our ability to test new areas with confidence. In particular, annual variation in phenology appears to influence vegetation indices derived from optical satellite systems (e.g., the enhanced vegetation index) and impacts accurate model classification of unlogged forested areas.

In the coming months we will be incorporating C-, L-, and X-band radar datasets from Sentinel-1, ALOS-2, and TanDEM-X in the hopes of improving classification on logged and unlogged areas.

Key results and impacts

The rapid depletion of forests has severe implications for global climate change, local populations and biodiversity. Estimating the amount of degraded forest is a missing piece in understanding the terrestrial portion of the global carbon budget. In addition, NGOs and global conservation initiatives, like the United Nation's Reducing Emission from Deforestation and forest Degradation (REDD+), actively seek monitoring systems that assess changes to forest structure.

Figure 1: The canopy gap

Figure 2: The closed canopy

THE INTERNATIONAL SYMPOSIUM ON DATA ASSIMILATION

Alison Fowler

The Fifth Annual International Symposium on Data Assimilation was held at the University of Reading during a very hot week in July 2016. This symposium brought together 200 scientists from over 15 countries spread across four different continents and received sponsorship from NCEO, the Met Office and ECMWF (The European Centre for Medium-Range Weather Forecasts).

This symposium comprised of 10 different sessions, one of which focused on the particular problem of assessing the value of observations. This is important not only for evaluating which (of the very many) observations are most important for providing an accurate weather forecast but also for designing instruments which are able to further reduce the uncertainty in the forecast. This latter problem is particularly difficult due to the fast pace at which data assimilation systems are changing, which means that by the time the instrument is operational (possibly in a few decades time) its value may be very different than if the data could be assimilated today.

The value of future observations

The atmosphere and oceans are being routinely observed by a myriad of instruments. These instruments are positioned on board orbiting satellites, aircrafts and ships, surface weather stations, and even balloons. The information collected by these instruments can be used to ensure that modelled weather forecasts adhere to reality using a process known as data assimilation.

For the observations to be useful it is necessary that:

- the observations can be compared to the forecast variables (e.g. temperature, humidity and wind)
- we know the uncertainty in those observations
- we know the uncertainty in the weather forecast model itself (so we know how much to trust the forecast vs how much to trust the observations).

These fundamentals of data assimilation are continually evolving, as the weather models become more sophisticated and are addressing new societal needs, new instruments are developed and computational resources and mathematical techniques advance.

There are many possible metrics for assessing the value of observations. Some are based on how sensitive the forecast skill is to the value of the observations, others try to quantify the amount of information in the observations for reducing the uncertainty in our knowledge of the current state of the atmosphere. Computing these metrics before the instrument is built and the data is available relies on accurate estimates of the error characteristics of the instrument and its relationship to the model variables and, hence, is very challenging.

It is clearly difficult to describe the value of a future observation unequivocally by a single figure. Instead we need to provide insight, through on-going research, as to how the value of observations is sensitive to changes in the ever evolving data assimilation system. There will be much to discuss at the next symposium!

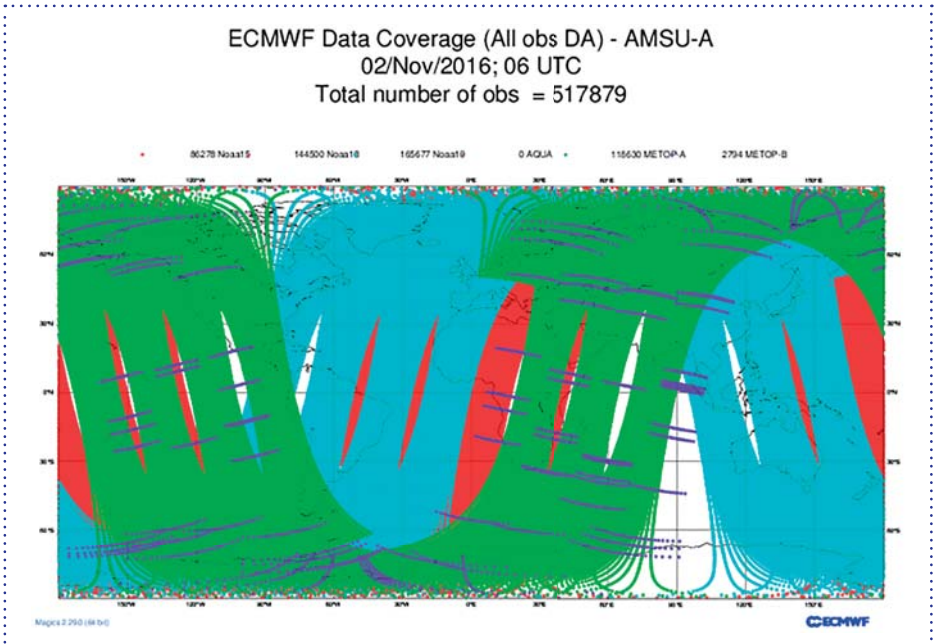

Figure 1: Data coverage of the AMSU-A instrument, on board 6 different satellites, within a 6 hour time window (copyright ECMWF)

EO DETECTIVE: BRINGING EARTH OBSERVATION INTO THE CLASSROOM AND BEYOND

Catherine Fitzsimons and Rosie Leigh, NCEO Leicester

The initial aim of the EO Detective project was to use Tim Peake's Principia mission to the International Space Station (ISS) to maximise the impact and engagement of the public with space and environment through Earth-observation-themed outreach activities. In 2015–16, with funding from the UK Space Agency and NERC, we developed a range of classroom resources and ran a competition for children aged 7–16.

The **resources** were highlighted on the Principia mission website and made available by ESERO-UK from October 2015. At least 600 teachers had downloaded one or more activities by June 2016. Some of the resources were also distributed in paper form to primary schools through the Tim Peake Primary Project (TPPP), and sample activities were available on the Principia website – so our estimate that they were used with 10,000 children is extremely conservative.

The EO Detective **competition** prize was the opportunity to have a photograph taken from the ISS. It was launched at the Royal Institution on 24 October 2015 and prizes were presented by Libby Jackson, the UK Space Agency's Astronaut Flight Education Programme Manager, at the National Space Centre on 1 October 2016. Entrants had to explain where on Earth they would like an astronaut to photograph and why. There were around a thousand interesting and varied entries, and an extra category had to be added for younger children. There is a list of winners and runners-up below. You can see the pictures on pages 42-43 and there are more details on the **EO Detective blog**.

The EO Detective 'team' have run workshops or activities at several **events**, including Launch Day celebrations in London and Leicester, the Big Bang Fair in Birmingham and the public days of the Farnborough International Air Show. We interacted with thousands of children and adults – attendance over the four days of the Big Bang Fair alone was 80,000 – introducing them to space photography and satellite imagery.

The resources remain relevant, and are being promoted by our **@EODetective** Twitter account and on the Principia website as well as being taken into a further 750 schools by TPPP. We have received additional funding from the UK Space Agency to create materials for younger children, a careers resource, and activities that children will be able to take home or access independently, so giving them the opportunity to engage parents, siblings and their wider social network in exploring Earth observation images.

EO Detective blog: eodetective.wordpress.com

Principia Mission website: principia.org.uk

National STEM Centre/ESERO-UK Tim Peake page: stem.org.uk/esero/tim-peake

Competition winners (winning images are overleaf) and * picture acknowledgements

1. The winners and runners-up in the EO Detective Competition display their prizes at the National Space Centre. Credit: National Space Centre. *National Space Centre.
2. Winning image for age 14–16: Fair Oaks, Indiana, methane emissions near pig farms. *Contains modified Copernicus Sentinel data 2016.
3. Winning image for age 11–14: Al Zaatari Refugee Camp Jordan, to compare with how it looked nearer the start of the conflict. *Earth Science & Remote Sensing Unit, NASA Johnson Space Centre.
4. Winning image for age 7–11: Lake Eyre, South Australia – to see what it looks like, full for the first time in years, *ESA/NASA.
5. Winning image for age 4–7: Rainforest near Manus, Brazil – to see how we are looking after the trees *Contains modified Copernicus Sentinel data 2016.
6. Runner up image for age 14–16: The Great Green Wall, Senegal – to see if it is affecting temperature and soil moisture levels. *Earth Science & Remote Sensing Unit, NASA Johnson Space Centre.
7. Runner up image for age 11–14: Inle Lake, Burma – to see if global warming and increasing tourism have affected water levels and the region around the lake. *Earth Science & Remote Sensin Unit, NASA Johnson Space Centre.
8. Runner up image for age 7–11: Central Beijing at night – to look at light pollution. *ESA/NASA.
9. Runner up image for age 7–11: Leticia and Tabatinga, meeting of three countries in the Amazon – to see if you can see differences in deforestation between the countries. *USGS/NCEO.
10. Runner up image for age 4–7: Angel Falls, Venuzuela – to find out if they are visible and if you can see how fast the water flows. *Japan Aerospace Exploration Agency (JAXA).
11. Runner up image for age 4–7: Pyramids – to show his teacher you can see man-made things from space and look at swirling sand. *ESA/NASA.
12. Runner up image for age 4–7: Knysna, South Africa – to see if it's possible to see the elephants in the forest. *Earth Science & Remote Sensing Unit, NASA Johnson Space Centre.
13. Tim Peake with EO Detectives Catherine Fitzsimons and Rosie Leigh. *NCEO.

1

2

3

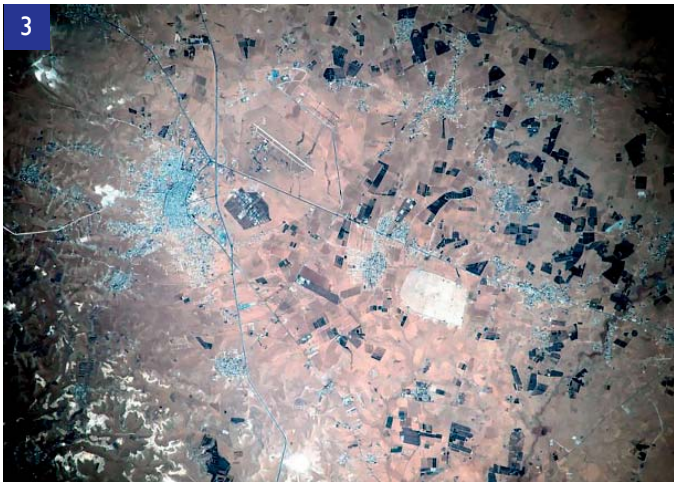

4

5

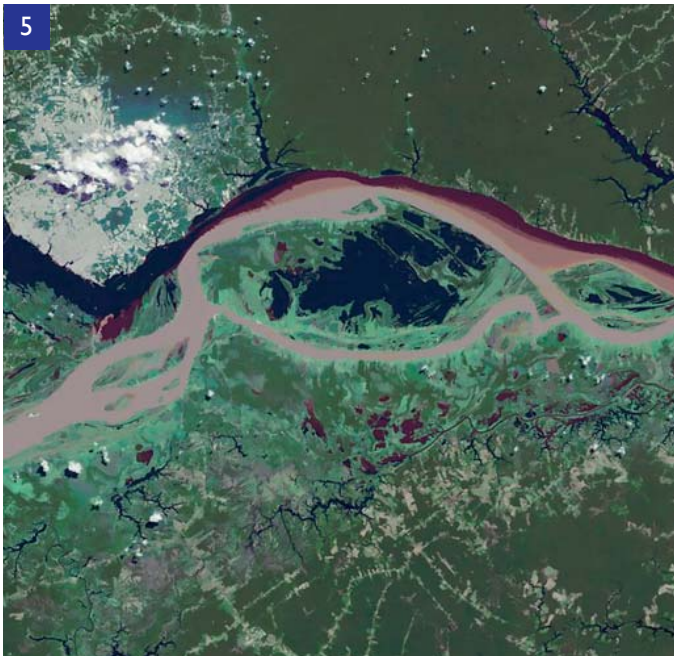

6

7

8

9

10

11

12

13

National Centre for Earth Observation
NATURAL ENVIRONMENT RESEARCH COUNCIL

NERC
SCIENCE OF THE ENVIRONMENT

John Remedios, NCEO Director
jjr8@leicester.ac.uk
National Centre for Earth Observation,
Michael Atiyah Building, University of Leicester,
University Road, Leicester, LE1 7RH, UK
Tel: +44 (0)116 252 2016
Fax: +44 (0)116 252 2464

Jan Fillingham, NCEO Training,
Communications and Events Manager
jan.fillingham@nceo.ac.uk
University of Reading, Earley Gate,
Building 58, Reading, RG6 6BB, UK
Tel: +44 (0)118 378 6728

Email info@nceo.ac.uk
Twitter @NCEOscience

www.nceo.ac.uk